



## Combretastatin-like chalcones as inhibitors of microtubule polymerisation. Part 2: Structure-based discovery of alpha-aryl chalcones

Sylvie Ducki<sup>a,b,c,d,\*</sup>, Grant Mackenzie<sup>c</sup>, Ben Greedy<sup>e</sup>, Simon Armitage<sup>e</sup>, Jérémie Fournier Dit Chabert<sup>c,d</sup>, Elizabeth Bennett<sup>c</sup>, Jim Nettles<sup>f</sup>, James P. Snyder<sup>f</sup>, Nicholas J. Lawrence<sup>a,e,\*</sup>

<sup>a</sup> Department of Chemistry, UMIST, Manchester M60 1QD, UK

<sup>b</sup> CRC Drug Development Group, Paterson Institute for Cancer Research, Christie Hospital NHS Trust, Manchester M20 4BX, UK

<sup>c</sup> Centre for Molecular Drug Design, University of Salford, Manchester M5 4WT, UK

<sup>d</sup> Laboratoire de Chimie des Hétérocycles et des Glucides, ENSCCF, Clermont Université, 63174 Aubière, France

<sup>e</sup> Drug Discovery Program, H. Lee Moffitt Cancer Center & Research Institute, Department of Interdisciplinary Oncology, University of South Florida, Tampa, FL 33612, USA

<sup>f</sup> Department of Chemistry, Emory University, 1515 Dickey Drive, Atlanta, GA 30322, USA

### ARTICLE INFO

#### Article history:

Received 15 July 2009

Revised 10 September 2009

Accepted 21 September 2009

Available online 2 October 2009

#### Keywords:

Chalcone  
Tubulin  
Combretastatin  
Colchicine  
Podophyllotoxin  
Antivascular  
Anticancer  
Docking

### ABSTRACT

Tubulin is an important molecular target in cancer chemotherapy. Antimitotic agents able to bind to the protein are currently under study, commonly used in the clinic to treat a variety of cancers and/or exploited as probes to investigate the protein's structure and function. Here we report the binding modes for a series of colchicinoids, combretastatin A4 and chalcones established from docking studies carried out on the structure of tubulin in complex with colchicine. The proposed models, in agreement with published biochemical data, show that combretastatin A4 binds to the colchicine site of  $\beta$ -tubulin and that chalcones assume an orientation similar to that of podophyllotoxin. The models can be used to design a new class of podophyllotoxin mimics, the  $\alpha$ -aryl chalcones, capable of binding to the colchicine-binding site of  $\beta$ -tubulin with higher affinity.

© 2009 Elsevier Ltd. All rights reserved.

### 1. Introduction

Tubulin has become an important target in cancer chemotherapy.<sup>1</sup> The heterodimeric protein plays an important role in the formation of the mitotic spindle, which provides the structural framework (microtubule) for the physical segregation of the chromosomes during mitosis. Drugs that interfere with the protein's dynamic stability are currently under study, commonly used in the clinic to treat a variety of cancers or exploited as probe to investigate the protein's structure and function. Three binding sites have been identified, named taxane, vinca alkaloid and colchicine **1**, after the ligands that occupy them. While agents populating the taxane pocket, such as paclitaxel, induce the assembly of microtubules and stabilise them, ligands occupying either the vinca alkaloid or the colchicine-binding sites inhibit the assembly of the protein into its polymer. These antimitotic agents have generated considerable interest due to the tremendous success of the

taxanes and vinca alkaloids in clinical oncology. Interest in these agents has been raised further by the discovery that combretastatin A4 (CA4 **2**) displays potent and selective toxicity towards tumour vasculature.<sup>2,3</sup> This effect is most pronounced for agents that bind at the colchicine-binding site.<sup>4</sup> Combretastatin A4 phosphate (CA4P **3**), a water soluble prodrug of CA4, is currently in phase III clinical trials for the treatment of cancer and early results are very promising.<sup>5</sup> Antimitotic agents able to target the colchicine-binding site have regained pharmaceutical interest and according to the National Cancer Institute (NCI), they are considered as important lead structures for the development of new anti-tumour agents.<sup>6</sup>

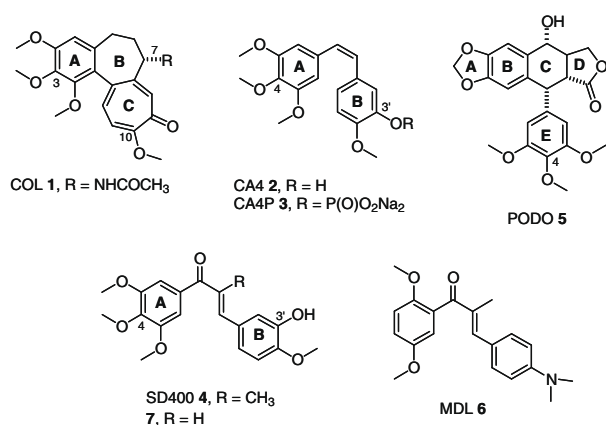
Our group has developed chalcones as an important class of antimitotic agents.<sup>7</sup> The lead compound, 4-hydroxyphenylbutenone, was isolated from the Chinese mint, *Scutellaria barbata*.<sup>8</sup> A comprehensive structure–activity relationship (SAR) study was conducted which led to the discovery of the chalcones which were found to inhibit tubulin assembly by binding to the colchicine-binding site of tubulin.<sup>9,10</sup>  $\alpha$ -Methyl chalcone SD400 **4** was found to be the most active compound of the series (inhibition of tubulin assembly, IC<sub>50</sub> 1.8  $\mu$ M for **4** vs 1.3  $\mu$ M for **2** and 2.6  $\mu$ M for **1**).

\* Corresponding authors.

E-mail addresses: [Sylvie.DUCKI@univ-bpclermont.fr](mailto:Sylvie.DUCKI@univ-bpclermont.fr) (S. Ducki), [Lawrennj@mitt.usf.edu](mailto:Lawrennj@mitt.usf.edu) (N.J. Lawrence).

$\alpha$ -Methyl chalcone **4** inhibits cancer cell growth at nanomolar concentrations [ $IC_{50}$  (K562) 0.21 nM for **4** compared to 1.4 nM for **2**] and binds to the colchicine-binding site of isolated tubulin ( $[^3H]$  colchicine remaining bound after drug competition 92%, same as CA4 **2**).<sup>10</sup>

In 1998, Nogales reported the 3.7 Å structure of the  $\alpha\beta$ -tubulin-paclitaxel complex, obtained by electron crystallography (EC) of zinc-induced tubulin sheets, providing a much awaited insight into the protein's structure and function.<sup>11</sup> Ravelli et al. later determined the 3.5 Å structure of tubulin in complex with DAMA-colchicine and with the stathmin-like domain (SLD) of RB3 clearly showing the location of the binding site and the conformation adopted by colchicine.<sup>12</sup> This model provides a structural framework for understanding the inhibition of tubulin assembly and its regulation by antimetabolic agents at the molecular level. Our contribution to this understanding recently resulted in a 5D-QSAR model able to predict the biological activity of agents binding to the colchicine-binding site.<sup>13</sup>



We now wish to report on the binding mode of a series of molecules able to occupy the colchicine-binding site. Colchicinoids, podophyllotoxin, combretastatin A4 and a series of chalcones were docked into the colchicine-binding site of tubulin reported by Ravelli et al. (PDB 1SA0). The models were examined and correlated with observed biochemical evidence to ascertain their reliability. The models were used to design a new class of podophyllotoxin mimics, the  $\alpha$ -aryl chalcones, capable of binding to the colchicine-binding site, causing G<sub>2</sub>/M arrest and inhibiting tubulin assembly.

## 2. Results and discussion

### 2.1. The colchicine-binding site

The antimetabolic agent, colchicine (COL **1**), binds to  $\beta$ -tubulin and inhibits tubulin assembly. Since this observation in the early 1970s, the mechanistic details of this interaction have often been addressed. Although the general toxicity of COL has hampered its use in cancer chemotherapy, a large number of analogues have been prepared and evaluated for their ability to inhibit tubulin assembly in vitro, providing a useful insight into the QSAR (quantitative structure–activity relationship) of this class of ligands.<sup>14</sup> Until recently attempts at localising the colchicine-binding site in the tubulin dimer had led to conflicting results.<sup>15,16</sup>

The report of the structure of paclitaxel-stabilised  $\alpha,\beta$ -tubulin by electron crystallography in 2001 by Nogales (PDB 1JFF)<sup>17</sup> raised interest in the use of computer modelling techniques to give an structural insight into the protein. In 2004, Ravelli et al. reported the structure of tubulin in complex with DAMA-colchicine and with the stathmin-like domain (SLD) of RB3 (PDB 1SA0), at 3.5 Å resolution.<sup>12</sup> The structure shows the interaction of the RB3-SLD

with two tubulin heterodimers capped at the top, suggesting that the microtubule regulatory role of stathmin is achieved by sequestering tubulin heterodimers, not allowing their incorporation into the microtubule. The structure locates the colchicine-binding site at the  $\alpha/\beta$  interface on the  $\beta$ -subunit. This structure (1SA0) differs substantially from the structure obtained by Nogales (1JFF). The tubulin dimer is in a straight conformation in 1JFF and a curved conformation in 1SA0. The colchicine-binding site in 1SA0 is mostly buried in  $\beta$ -tubulin, in a previously inaccessible domain in 1JFF. As a consequence this area was not considered in our initial assessment of 1JFF for potential colchicine-binding sites (results unpublished). Strands S8 and S9, loop T7 and helices H7 and H8 of  $\beta$ -tubulin surround DAMA-colchicine, which also interacts with loop T5 of the neighbouring  $\alpha$ -subunit.

In order to check that the selected docking process was adequate for finding the correct binding mode of ligands binding to the colchicine-binding site, colchicine was extracted from the original structure (1SA0) and re-docked using AUTODOCK.<sup>18</sup> The binding mode of the lowest energy complex, post-docking minimisation, was compared to the crystal structure (Fig. 1). The docking study using AUTODOCK results in a binding mode for colchicine that is almost identical to that found in the original X-ray structure (rms 0.7 Å between the best scored conformers from docking and X-ray structure 1SA0). The structure correlates well with biochemical data showing that  $\beta$ 318 tubulin isoforms have a reduced sensitivity to colchicine and data by Bai showing that the C2-oxygen atom of colchicine is close to Cys $\beta$ 241 and the C3-oxygen atom is close to Cys $\beta$ 356.<sup>19</sup>

### 2.2. The podophyllotoxin binding site

Ravelli et al. also determined the 4.2 Å structure of the ternary tubulin:podophyllotoxin:RB3-SLD complex (PDB 1SA1) and found that podophyllotoxin (PODO **5**) binds to tubulin at the same site as COL **1** but adopts a different orientation.<sup>12</sup> The binding mode for PODO **5** was also evaluated using the procedure described above and compared to the binding mode published by Ravelli et al. (Fig. 2). It is important to note here that the docking was

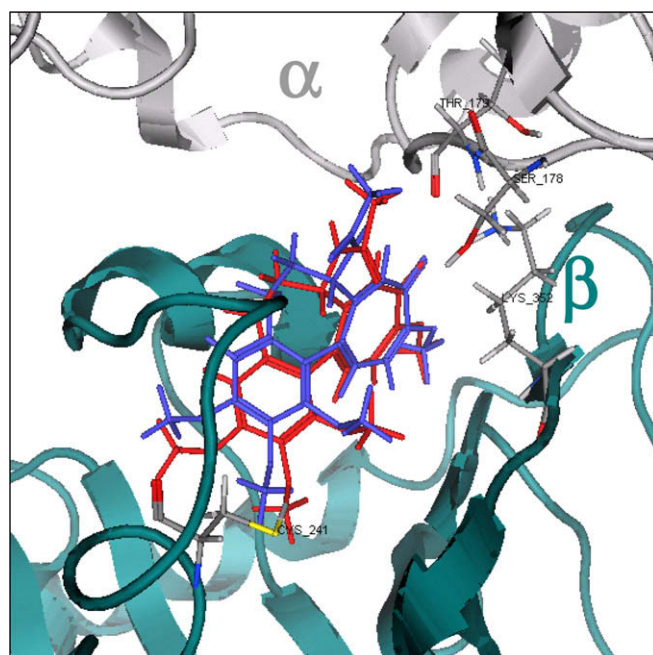


**Figure 1.** Comparison of X-ray (PDB 1SA0; red) and docked (blue) COL **1** (rms 0.7 Å).

non-biased; no preliminary superposition was carried out. The docked structure of PODO **5** was found to be very similar to the original X-ray structure (rms 1.5 Å between the best scored conformers from docking and X-ray structure 1SA1).

It was not surprising to find that the trimethoxyphenyl ring of COL **1** and PODO **5** are both buried in a hydrophobic pocket in  $\beta$ -tubulin,<sup>20</sup> surrounded by Cys $\beta$ 241, Ala $\beta$ 250, Leu $\beta$ 252, Leu $\beta$ 255, Ala $\beta$ 354 and Cys $\beta$ 356. Various biochemical experiments had come to this conclusion, including Chaudhuri, who found that both COL **1** and PODO **5** could inhibit the formation of crosslinks between Cys $\beta$ 241 and Cys $\beta$ 356 by EBL.<sup>21</sup> Although both COL and PODO populate the same pocket on  $\beta$ -tubulin, the molecules do not completely overlap in the binding site. This had been observed in competition studies where *N*-acetyl mescaline (NMA) presented a high affinity for tubulin binding but was inhibited by both COL and PODO and tropolone methyl ester (TME) had been shown to inhibit COL but not PODO binding. These results suggested both ligands shared the site where the trimethoxyphenyl ring bound, but differed in other binding features.<sup>22,23</sup>

### 2.3. Docking of combretastatin A4

Since its discovery in 1989,<sup>24</sup> CA **2** and its analogues have had tremendous coverage in the literature for their ability to inhibit tubulin assembly by binding to the colchicine-binding site.<sup>25–27</sup> Several structure-based models have been developed to elucidate important structure–activity relationship for the combretastatins.<sup>28,29</sup> In 2005, Kong et al. described a molecular model for tubulin–combretastatin interactions and used it to design boronic acid bioisosteres of CA **4**.<sup>30</sup>

CA **2** was docked into the colchicine-binding site using our docking methodology. AUTODOCK scores and visual inspection allowed us to select the most probable binding mode (Fig. 3). Although rings A and B of CA **4** and rings A and C of COL occupy similar orientation, CA **4** appears to fit deeper into the  $\beta$ -subunit of tubulin than in Kong's proposed binding model. The three methoxy groups in CA **4** are 6.12, 3.61 and 3.33 Å (3-O $\cdots$ S, 4-O $\cdots$ S and 5-O $\cdots$ S, respectively) from Cys $\beta$ 241, while the three methoxy

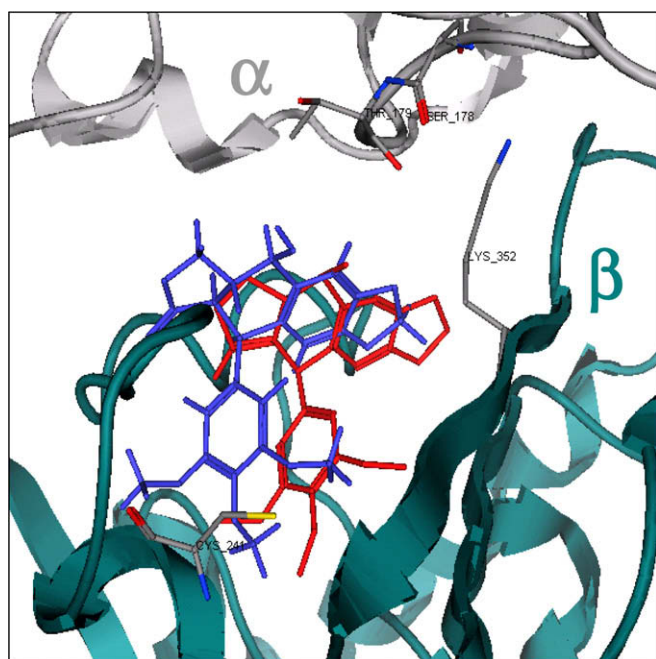


**Figure 2.** Comparison of X-ray (PDB 1SA1; red) and docked (blue) PODO **5** (rms 1.5 Å).

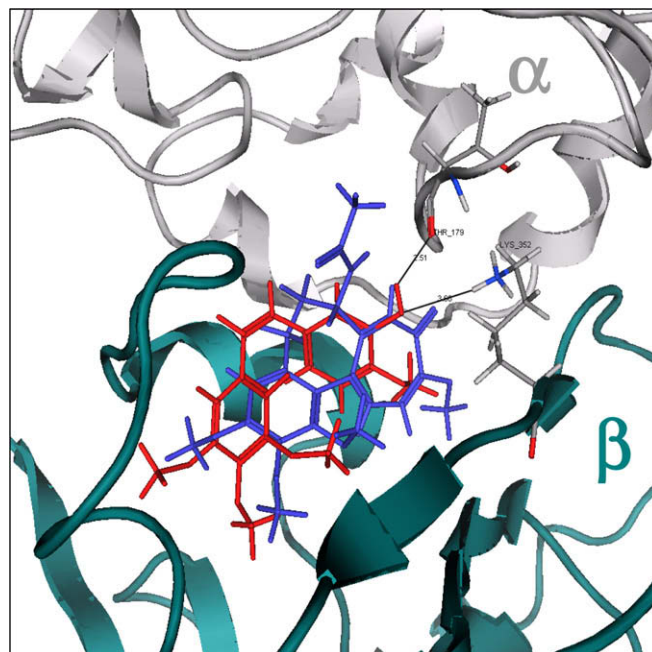


**Figure 3.** Comparison of CA **4** (red) and COL (blue) binding models with tubulin (PDB 1SA0).

groups of COL in 4.16, 3.25 and 5.44 Å (2-O $\cdots$ S, 3-O $\cdots$ S and 4-O $\cdots$ S, respectively) away from the same residue. Our model also shows that the 3-hydroxyl group of the B-ring of CA **4** is in close proximity to the carbonyl group of Thr179 of the  $\alpha$ -tubulin subunit, and that these may be involved in a hydrogen bond (O $\cdots$ O 3.05 Å). The model also suggests that this hydroxyl moiety might be involved in a hydrogen bond with the backbone of Lys352 on  $\beta$ -tubulin (O $\cdots$ N 4.59 Å), which is consistent with the fact that CA **4** induces GTPase activity.<sup>31</sup> The same hydrogen bond is observed with the C-10 carbonyl of COL analogues (O $\cdots$ N 2.88 Å) that induce the GTPase activity of the enzyme. Nguyen et al. recently reported that the binding mode of CA **4** was very similar to COL and that the two ligands belonged the same pharmacophore group, which is consistent with our finding.<sup>32</sup>

### 2.4. Docking of chalcones

Peyrot et al. reported that *trans*-1-(2,5-dimethoxy)-3-[4-(dimethylamino)phenyl]-2-methyl-2-propen-1-one (MDL **6**) was a powerful antimetabolic agent, binding rapidly and reversibly to the colchicine-binding site of tubulin<sup>33</sup> while our group recently reported that both chalcones MDL **6** and SD400 **4** were able to bind to the colchicine-binding site of  $\beta$ -tubulin, inhibiting its assembly into microtubules.<sup>10</sup> MDL and SD400 were docked into the colchicine-binding site using our docking methodology. AUTODOCK scores and visual inspection allowed us to select the most probable binding mode. Both chalcones displayed very similar binding modes (Fig. 4).

The proposed binding site for MDL and SD400 is located on  $\beta$ -tubulin, at the interface with the  $\alpha$ -subunit. The polymethoxyphenyl ring of the three ligands (SD400, PODO and COL) adopt very similar orientation, close to Cys $\beta$ 241 (SD400 4-O $\cdots$ S = 3.45 Å, PODO 4-O $\cdots$ S = 3.40 Å, COL 3-O $\cdots$ S = 3.25 Å) which is not surprising since the binding of chalcones can be inhibited by COL, MTC and PODO. The importance of this trimethoxyphenyl moiety in agents interacting with the colchicine-binding site of tubulin has already been observed.<sup>1</sup> In this model, we observe that the enone bridge between the two aromatic moieties of the chalcone does

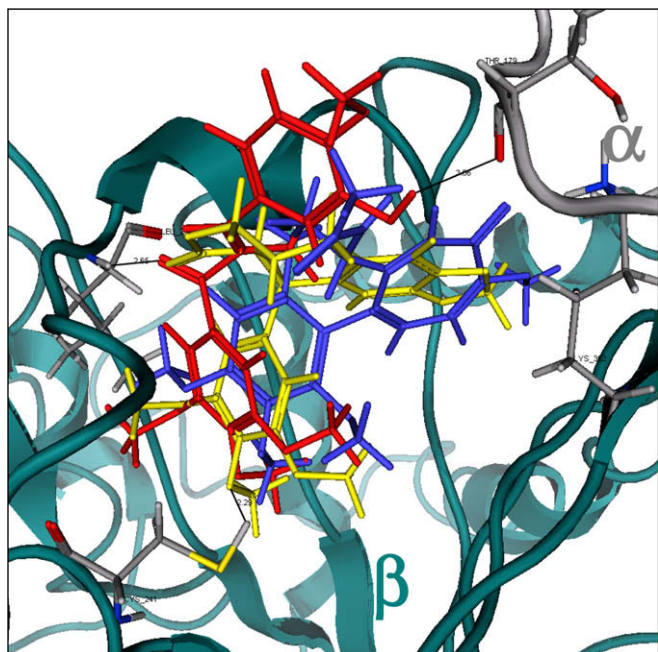


**Figure 4.** Comparison of SD400 (red), COL (blue), PODO (yellow) binding models with tubulin (PDB 1SA0).

not overlap COL or CA4, but has the same orientation as the D-ring of PODO **5**. The C=O of enone **4** even resembles the position of the C=O of PODO **5** (ring D), and the model suggests that it might be involved in a hydrogen bond with the backbone of Asp-251 in  $\beta$ -tubulin ( $C=O_{SD400} \cdots H-N_{Asp-251} = 2.18 \text{ \AA}$  and  $C=O_{PODO} \cdots H-N_{Asp-251} = 4.07 \text{ \AA}$ ). The importance of this ketone is consistent with our observation that reduction to its 1-OH analogue resulted in reduced cytotoxicity against the human K562 cell line (SD400 **4**: $IC_{50}$  of 0.21 nM vs 1-OH analogue: $IC_{50}$  of 90 nM) and loss of ability of inhibit tubulin assembly (SD400 **4**: $IC_{50}$  of 0.46  $\mu\text{M}$  vs 1-OH analogue: $IC_{50}$  of  $>10 \mu\text{M}$ ).

The arrangement of ring C of COL and ring B of CA4 within the binding pocket (close to Leu-352 on  $\beta$ -tubulin) has been associated with induction of GTPase activity, presumably due to a conformational change caused by interaction with this part of the binding pocket. Since MDL was shown to induce no GTPase activity, we were not surprised to observe that neither SD400 nor MDL bound to this region of the binding site. Instead the chalcones preferred to adopt a conformation which favoured a hydrogen bond between the 3'-hydroxyl moiety (ring B) and the C=O of Thr179 on  $\alpha$ -tubulin ( $O-H \cdots O=C$  3.00  $\text{\AA}$ ), much like the hydroxyl group on ring C of PODO ( $O-H \cdots O=C$  3.54  $\text{\AA}$ ), which was also shown to induce no GTPase activity.

The bioactive conformation adopted by the chalcones is worth further discussion. We previously reported that SD400 **4** was more active than its  $\alpha$ -demethylated analogue **7**.<sup>9,13</sup> The minimum *s-cis* and *s-trans* conformations for both systems were optimised using the HF/6-31\* level of theory in PC GAMESS version of the GAMESS (US) QC package. The results of these calculations indicate that the *s-cis* conformation (torsion angle O–C1–C2–C3 of the enone system is 37.6°) is favoured by 2.30 kcal mol<sup>-1</sup> in the case of chalcone **7**, but that the *s-trans* conformation (torsion angle O–C1–C2–C3 of the enone system is 146.1°) is favoured by 1.85 kcal mol<sup>-1</sup> for the  $\alpha$ -methyl chalcone **4**. We therefore attribute this difference in activity to the fact that SD400 **4** prefers to adopt a bioactive conformation closer to a *s-trans* conformation while chalcone **7** prefers the energetically less demanding *s-cis* conformation. This choice in conformation is ideal for SD400 as it allows additional interaction

with the protein through the 3'-OH group (ring B). The fact that the analogues substituted with methoxy-, hydrogen or fluoro- at the 3'-position weakly inhibit tubulin assembly reinforces the importance of this group and its spatial location in the ligand. We have already demonstrated the importance of this hydroxyl group in our QSAR study.<sup>13</sup>

## 2.5. Structure-based design

The models presented suggest that CA4 binds to  $\beta$ -tubulin in a similar orientation as COL, whereas the chalcones' binding mode was similar to that of PODO. CA4 and COL would therefore belong to a different pharmacophore group than chalcones and PODO. The model also suggests that the addition of a planar hydrophobic moiety, such as a phenyl ring C, at the  $\alpha$ -position of the chalcone skeleton would mimic ring B of podophyllotoxin very well (Fig. 5).

## 2.6. Synthesis of $\alpha$ -aryl chalcones

Two routes were used to prepare the alpha-aryl chalcones. In the first route (Scheme 1), alpha-aryl chalcones **12** were prepared as single isomers through a Suzuki coupling while the second route (Scheme 2) provided alpha-aryl chalcones **13** as mixtures of *E/Z* isomers.

Chalcones **8a–c** were obtained by condensation of 3,4,5-trimethoxyacetophenone and substituted benzaldehydes **9a–c** in sodium hydroxide/methanol in high yields (82–95%). In the case of chalcone **8c**, the hydroxyl group was protected as a silyl ether with TBDMSCl to give chalcone **8d** (85% yield). Bromination ( $\text{Br}_2$ ,  $\text{Et}_3\text{N}$ ) of chalcones **8a–b,d** afforded  $\alpha$ -bromo-chalcones **10a–c** (44–73%), which underwent a Suzuki coupling with substituted phenyl boronic acids **11a–f** to provide alpha-aryl chalcones **12a–h** in moderate to good overall yields (26–84%) with high selectivity for the *E*-isomer in all cases. The silyl protecting group of **12c** was cleaved with TBAF to afford alpha-aryl chalcone **12i** in 95% yield.

The preparation of alpha-aryl chalcones **13a–o** was achieved by Knoevenagel condensations of a range of substituted benzaldehydes **9a–d** with ketones **14a–c** using piperidine as a base in excellent yields (58–97%). The products from these reactions were isolated as *E/Z* mixtures. Ketones **14a–c** were prepared by Grignard addition of substituted benzyl halide **15a–c** to 3,4,5-trimethoxybenzaldehyde followed by PCC oxidation of the alcohol **16a–c** (53–73% over two steps).

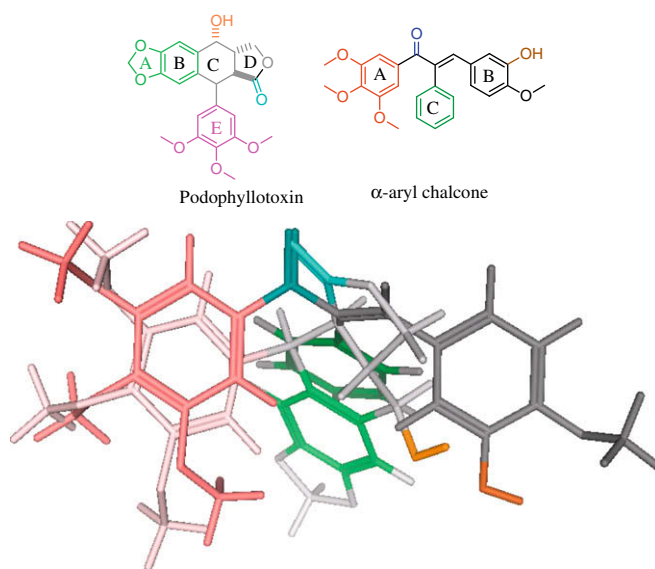
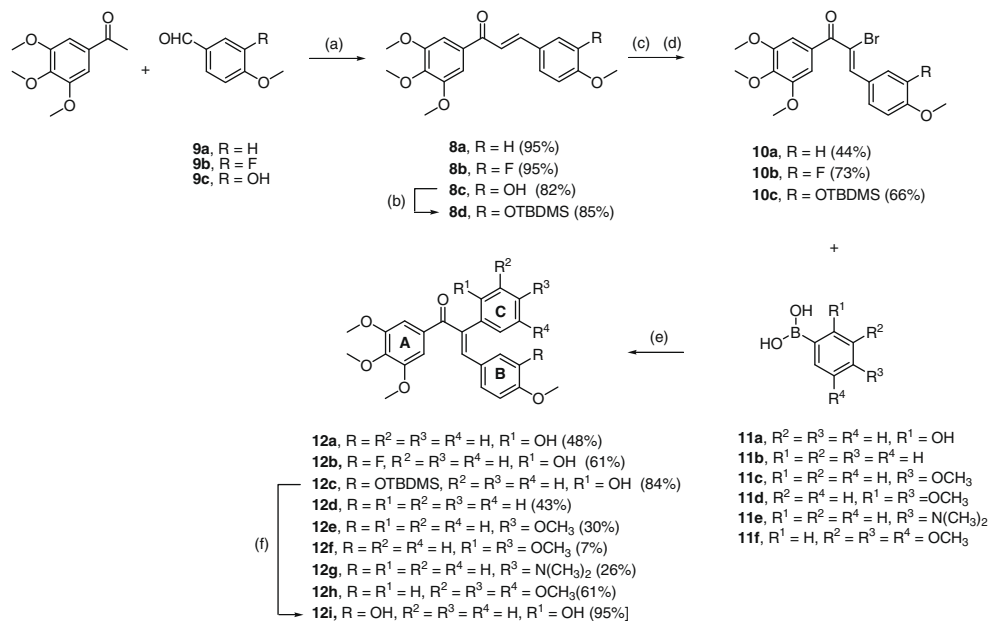
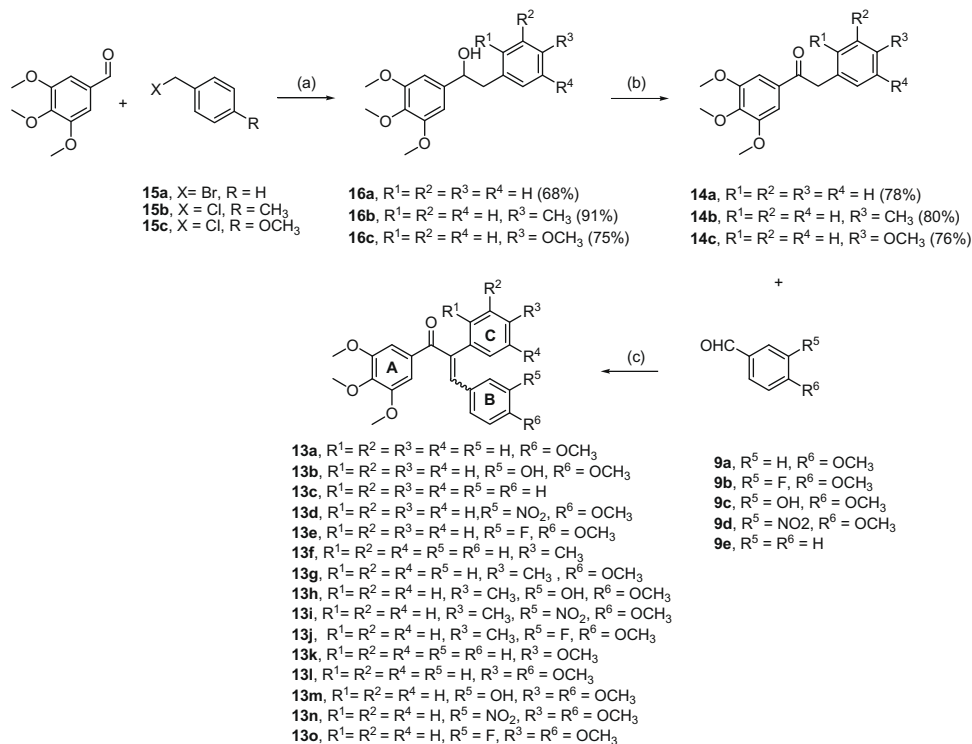


**Figure 5.** Pharmacophoric Points between podophyllotoxin and  $\alpha$ -aryl chalcones.



**Scheme 1.** Reagents and conditions: (a) 50% NaOH, MeOH, rt, 16 h; (b) TBDMSCl, *i*Pr<sub>2</sub>EtN, DMF, reflux, 1 h; (c) Br<sub>2</sub>, CHCl<sub>3</sub>, 0 °C; (d) Et<sub>3</sub>N, reflux; (e) Ar-B(OH)<sub>2</sub> **11a–f**, Pd<sub>2</sub>(dba)<sub>3</sub>, PPh<sub>3</sub>, Et<sub>2</sub>NH, Tol/*n*-PrOH; (f) TBAF, THF, rt, 30 min.



**Scheme 2.** (a) Mg, THF, reflux, 1 h; (b) PCC, DCM, rt, 3 h; (c) piperidine, benzene, reflux, 6–8 h.

## 2.7. Biological evaluation

Chalcones **12–13** were first assessed *in vitro* for their ability to inhibit cell proliferation against the human leukaemia K562 cell line (Table 1).

As predicted by the model, the addition of the bulky phenyl ring C had no adverse effect on the biological activities of the chalcones and all analogues displayed potent bioactivity. The biological activ-

ity followed the same pattern as previously reported with regards to the substituents at position 3 on ring B, with hydroxylated analogues fifteen times more active than analogues bearing R = F or H, highlighting once again the importance of the 3-OH group on ring B.<sup>13</sup> The substitution pattern on ring C had little influence on the biological activity although less bulky substituents were preferred, as exemplified by **12f** bearing one methoxy group (IC<sub>50</sub> K562 = 90 nM) and **12h** bearing three methoxy moieties (IC<sub>50</sub>

**Table 1**

Inhibition of cancer cell proliferation against the K562 human leukaemia cell line (IC<sub>50</sub>, concentration required to inhibit 50% of cell proliferation), inhibition of tubulin assembly (IC<sub>50</sub>, concentration required to inhibit 50% of tubulin assembly)

Compd	Yield (%)	E/Z ratio	IC <sub>50</sub> (K562) nM	IC <sub>50</sub> (tubulin) μM
<b>12a</b>	48	1:0	370	>10
<b>12b</b>	61	1:0	60	7.2
<b>12c</b>	84	1:0	380	>10
<b>12d</b>	43	1:0	20	N.D.
<b>12e</b>	30	1:0	40	N.D.
<b>12f</b>	37	1:0	90	N.D.
<b>12g</b>	26	1:0	150	N.D.
<b>12h</b>	61	1:0	2200	N.D.
<b>12i</b>	95 from <b>12c</b>	1:0	49	5.5
<b>13a</b>	91	1.7:1	240	9.5
<b>13b</b>	74	1:0	35	N.D.
<b>13c</b>	80	1.4:1	6300	N.D.
<b>13d</b>	90	2:1	>10,000	N.D.
<b>13e</b>	87	1.5:1	790	N.D.
<b>13f</b>	93	2:1	2970	N.D.
<b>13g</b>	77	2:1	760	N.D.
<b>13h</b>	95	2:1	32	2.6
<b>13i</b>	58	7:6	2430	N.D.
<b>13j</b>	72	11:4	570	4.4
<b>13k</b>	97	1:1	4920	N.D.
<b>13l</b>	88	2:1	500	N.D.
<b>13m</b>	90	5:4	12	2.1
<b>13n</b>	67	4:1	2660	N.D.
<b>13o</b>	67	10:7	450	4.2
<b>4</b>		1:0	4.4	3.3
<b>2</b>		0:1	3.2	3.7

K562 = 2.2 nM). Since two routes were taken to prepare the alpha-aryl chalcones, we were also able to look at the influence of the configuration of the double bond. For example, chalcone **12d** (IC<sub>50</sub> K562 = 20 nM) was synthesised as a single *E*-isomer while chalcone **13a** (IC<sub>50</sub> K562 = 240 nM) was obtained as a 10:17 mixture of two isomers. It is clear, in this case, that the *E*-configuration of the double bond is preferred for high activity.

The conformation of the enone system has also been found to be an important factor for good activity. Here we designed 2-hydroxylated chalcone **12i**, where the 2-OH would be able to form an intramolecular hydrogen bond with the C=O of the enone hence favouring the *S-trans* configuration. However, compared to chalcone **13b** (IC<sub>50</sub> K562 = 35 nM), chalcone **12i** (IC<sub>50</sub> K562 = 49 nM) did not present any advantage in vitro. The most active chalcone of the series was found to be chalcone **13m** (IC<sub>50</sub> K562 = 12 nM). This activity represents that of the mixture of isomers since we did not manage to separate them. This chalcone is only three times less active than the most active chalcone reported so far, chalcone **2** (IC<sub>50</sub> K562 = 4.4 nM) and bears the 3-OH and 4-OCH<sub>3</sub> substituents on its B-ring and a 4-OCH<sub>3</sub> on its C-ring.

Selected α-aryl chalcones were evaluated for their ability to inhibit tubulin assembly in vitro (Table 1). Here again the analogues bearing 3-OH on ring B displayed the highest activity, with two analogues **13h** and **13m** more effective than SD400 **4** and CA4 **2**. These results prove that the cytotoxic effect of the α-aryl chalcones

is caused by their ability to bind to tubulin and inhibit its assembly into microtubules. It also shows that the addition of a phenyl ring alpha to the enone does not prevent the chalcone from binding to tubulin.

Chalcones **12b**, **12i** and **13m** were selected for further evaluation. The compounds were evaluated against a series of cell lines (murine leukaemia P388, human lymphoma L1210, human lung A549, human ovarian A2780), in which they displayed very potent activity, in the nanomolar range (Table 2).

Flow cytometry was then used to evaluate the effects of these agents on the growth and division of cells, by measuring the DNA content of eukaryotic cells (Table 2). It was evident that the cell population of the untreated cells predominantly resided in the G<sub>0</sub>-G<sub>1</sub>/S-phases of the cycle (77%). This contrasted significantly with cells treated with chalcones **12b**, **12i** and **13m** which appeared to act by blocking the cells in mitosis, illustrated through an accumulation of cells in the G<sub>2</sub>/M phase (46–75% compared to 23% for untreated cells). Such cells appeared to have the capacity to replicate their DNA but were incapable to proceed through the cell cycle to cell division. These results are consistent with those obtained for classical tubulin-binding drugs. We noted that the newly designed alpha-aryl chalcone **12i** was able to block the cell cycle in the G<sub>2</sub>/M phase more extensively than SD400 **4** and CA4 **2** (75% vs 56% and 63%).

### 3. Conclusion

Using an experimentally determined structure for the colchicine-binding site of tubulin as a template, we established the binding modes for a series of colchicinoids, podophyllotoxin **5**, combretastatin A4 **2** and chalcone SD400 **4** deduced from docking studies. Our models suggest that combretastatin A4 adopts a similar orientation to that of colchicine when bound to β-tubulin. Our modelling studies imply that the chalcones' binding mode is very similar to that of podophyllotoxin and that the two ligands would therefore belong to the same pharmacophore group. The model pointed toward the addition of a planar hydrophobic moiety, such as a phenyl ring, at the alpha position of the chalcone skeleton which would mimic ring B of podophyllotoxin very well.

We designed and synthesised a series of alpha-aryl chalcones **12–13** as mimics of podophyllotoxin to validate this model. During our modelling studies, we noted that the B-rings of both chalcones and combretastatin A4 did not occupy the same pocket in tubulin and belonged to different pharmacophore groups. We imagined that the alpha-aryl chalcones **12–13** could occupy both pockets and display synergistic activity. We found that chalcone **13m** displayed the highest bioactivity against cancer cells in vitro (IC<sub>50</sub> K562 12 nM). Also chalcone **13m** was able to inhibit tubulin assembly at a higher degree than the reference compounds **2** (IC<sub>50</sub> tubulin 3.3 μM) and **4** (IC<sub>50</sub> tubulin 3.7 μM). This chalcone has the 3-OH and 4-OCH<sub>3</sub> substituent on the B-ring, just like combretastatin A4 and chalcone **4**, while the C ring is substituted with a 4-OCH<sub>3</sub> and can be considered as chalcone:combretastatin hybrid compound.

**Table 2**

Inhibition of cancer cell proliferation (IC<sub>50</sub>, concentration required to inhibit 50% of cell proliferation), flow cytometry (cell distribution, % cells in G<sub>0</sub>/G<sub>1</sub>, S, G<sub>2</sub>/M phases)

Compd	Inhibition of cell proliferation IC <sub>50</sub> (nM)				Flow cytometry		
	P388	L1210	A549	A2780	G <sub>0</sub> /G <sub>1</sub>	S	G <sub>2</sub> /M
<b>12b</b>	530	60	140	40	10.6	43.6	45.7
<b>12i</b>	28	36	50	34	6.5	18.1	75.4
<b>13m</b>	20	160	680	10	10.8	34.6	54.6
<b>4</b>	26	11	10	1.8	10.7	32.8	56.4
<b>2</b>	3.1	2.3	7.8	1.9	14.0	23.3	62.7
Control					47.9	28.8	23.3

## 4. Experimental section

### 4.1. Molecular modelling

The BIOPOLYMER and SYBYL (Tripos, St. Louis) programs were used to build and visualise the models. All calculations in this work were performed on a 2.4 GHz Pentium IV processor running Windows 2000. The docking calculations were carried out using AUTODOCK 3.0.5.<sup>18</sup> Molecular mechanics calculations were performed using the Molecular Operating Environment (MOE) 2004.03 molecular modelling software. Quantum mechanical calculations were performed using the PC GAMESS version of the GAMESS (US) QC package.

#### 4.1.1. Preparation of the structure

The 3.58 Å structure of tubulin in complex with DAMA-colchicine and with the stathmin-like domain (SLD) of RB3 was downloaded (PDB 1SA0). Tubulin dimer 1 (chains A and B) was extracted along with the associated GTP, GDP, DAMA-colchicine and Mg. This was as the starting point for structural relaxation using the MMFF94 force field. There were several residues missing from the crystal structure due to weakly defined electron densities. These were residues 38–46 and 438–451 of  $\alpha$ -tubulin, and residues 278–285 and 439–455 of  $\beta$ -tubulin. Five percentage of the side chains were poorly defined and modelled as alanines in the downloaded structure. DAMA-colchicine, GTP and GDP were given the appropriate atom types; the Tripos force field atom types allocated to the protein by SYBYL were recognised and converted to MMFF94 atom types. The hydrogens were added using SYBYL'S BIOPOLYMER. The missing residues were added to the structure by homology to the equivalent residues in the minimised 1JFF structure. The minimised structure derived from 1JFF was aligned to the end of the chains of the missing residues to obtain the correct orientation. The required residues were extracted from the 1JFF structure and merged into the 1SA0 structure. These added residues were minimised to a RMS of 0.5 kcal mol<sup>-1</sup> using the MMFF94 force field and a distant dependant dielectric of 3. During the minimisation runs the rest of the system was held fixed as an aggregate. The missing side chains were then added by mutating the alanine residues to the required residue using the SYBYL BIOPOLYMER module. These were then minimised to a RMS of 0.05 kcal mol<sup>-1</sup> using the MMFF94 force field and a distant dependant dielectric of 3 while the rest of the system was held fixed as an aggregate. The relaxation of the crystal structure was approached in a step-wise manner using low-temperature dynamics to relieve bad contacts from the deposited crystal structure but to retain the secondary structure of the protein. The side chains were relaxed first with the rest of the atoms fixed as an aggregate. A constant dielectric of 78 is used to stop the electrostatic interaction between the charged side chains being exaggerated. The simulation of the protein is performed in a vacuum so this dielectric prevents the unrealistic movement of the side chains due to unshielded electrostatic interaction. The dynamics simulation was run in SYBYL 6.9 using the MMFF94 force field and charges. The simulation was run for 1000 fs within the NTV ensemble at a temperature of 20 K and a structure was extracted every 10 fs. The 140 fs structure was chosen to take to the next stage of the structure preparation. The energy had dropped from an initial potential energy of 37299.56 kcal mol<sup>-1</sup> using the current force field setup to 19200.40 kcal mol<sup>-1</sup>, while the RMSD of the side-chain atoms is only of 0.38 Å.

Using the structure from the last dynamics calculation as input, the next stage was to relieve bad contacts in the backbone of the protein. In this simulation the backbone atoms and all atoms within 2 Å of these were allowed to move with all others being held fixed. The dynamics simulation was run using the MMFF94 force field and charges with a distant dependant dielectric of 3. The sim-

ulation was run for 1000 fs within the NTV ensemble at a temperature of 20 K and a structure was extracted every 10 fs. The 140 fs structure was chosen to take to the next stage of the structure preparation. The energy had dropped from an initial potential energy of 17189.09 kcal mol<sup>-1</sup> using the current force field setup to 13955.73 kcal mol<sup>-1</sup>, while the RMSD of the atoms in the backbone is only 0.24 Å.

The next stage of the preparation of the deposited crystal structure was the relaxation of whole molecule when none of the atoms are held fixed. The dynamics simulation was run using the MMFF94 force field and charges with a distant dependant dielectric of 3. The simulation was run for 5000 fs within the NTV ensemble at a temperature of 20 K and a structure was extracted every 10 fs. The 240 fs structure was chosen to take to the next stage of the structure preparation. The energy had dropped from an initial potential energy of 13955.73 kcal mol<sup>-1</sup> using the current force field setup to 11520.24 kcal mol<sup>-1</sup>, while the RMSD of the atoms is 0.5 Å.

The final step of the preparation process was a full minimisation of the system. The MMFF94s force field and charges was used with a distant dependant dielectric of 3. The minimisation completed when the energy converged to a RMSD of 0.05 kcal mol<sup>-1</sup>. This minimised structure was chosen to be the final relaxed structure.

#### 4.1.2. Docking

The minimised structure was used in a series of docking calculations using the AUTODOCK 3.0.5 program. The coordinates of the minimised structure were used but the molecular partial charges were calculated with a different method. The scoring function used in AUTODOCK 3.0.5 is based on the Amber force field. Because of this it was decided that the use of Kollman ESP derived partial charges would be more appropriate. MOE was used to allocate the Kollman charges (AMBER 94 in MOE). AUTODOCK tools were then used to produce the required files for grid generation and running the AUTODOCK calculation. A grid of 60 × 60 × 60 was used to ensure that the area probed was adequate for the ligands to explore all possible binding modes. The AUTODOCK results were clustered using a RMS tolerance of 2.0 Å to distinguish between similar binding modes. Low energy binding modes and the lowest energy conformation from clusters of 5 or more occurrences were selected for further refinement. These were then refined using the MMFF94 force field, with the binding mode that had the lowest complex energy after minimisation being selected as the final binding mode taken forward for analysis and comparison to experimentally observed properties.

#### 4.1.3. Conformational search

Conformational searches for the ligands under investigation were performed with the stochastic search method, as implemented in MOE. In these calculations all rotational bond were rotated to a random dihedral angle with a bias added to select angles with a sum-of-gaussians distribution with peaks at multiples of 30°. Following the rotation of the bonds a dihedral minimisation was performed, to an RMS gradient of 100 kcal/mol Å, to relieve bad non-bonded contacts. Subsequent Cartesian minimisation, to an RMS gradient of 0.001 kcal/mol Å, generates the final conformation, which is checked to determine if it is unique by comparing all atom positions using an RMS tolerance of 0.1 Å. The procedure was terminated when the number of failures to find a new conformation exceeded 10,000 in a row and conformations with energies over 20 kcal/mol above the minima were rejected.

The quantum mechanical optimisation was performed in PC GAMESS using the restricted Hartree-Fock (RHF) Hamiltonian and Pople's 6-31G\* split valence basis set with polarisation functions on heavy atoms. Input coordinates were taken from the stochastic conformational searches.

## 4.2. Chemistry

400 MHz  $^1\text{H}$  and 100 MHz  $^{13}\text{C}$  NMR spectra were recorded using a Bruker AC 400 Spectrometer.  $^{13}\text{C}$  NMR spectra were recorded using Distortionless Enhancement by Polarisation Transfer. Both  $^1\text{H}$  and  $^{13}\text{C}$  spectra were recorded using  $\text{CDCl}_3$  as internal standard unless otherwise indicated. Chemical ionisation (CI) mass spectra were recorded using a Kratos MS25 mass spectrometer. Accurate mass determinations were carried out on a Kratos Concept IS spectrometer. Melting points were determined using an electrothermal melting point apparatus and were uncorrected. Column chromatography was conducted using Silica Gel 60 230–400 mesh (Merck & Co.). Silica TLC was conducted on pre-coated aluminium sheets (60 F254) with a 0.2 mm thickness (Aldrich Chemical Co.).

### 4.2.1. General procedure for the preparation of chalcones **8a–c**

A stirred solution of 3,4,5-trimethoxyacetophenone (12 mmol) and the substituted benzaldehyde **9a–c** (12 mmol) in methanol (30 mL) was treated at room temperature with a 50% methanol NaOH solution (1 mL) and the resulting solution stirred at room temperature for 24 h. The mixture was then acidified by addition of 1 N HCl and the crude product extracted into dichloromethane ( $3 \times 20$  mL). The organic phases were dried ( $\text{MgSO}_4$ ) and evaporated in vacuo. The resulting solid was recrystallised from methanol affording chalcones **8a–c** in excellent yields (82–95%).

**4.2.1.1. (E)-3-(4-Methoxyphenyl)-1-(3,4,5-trimethoxyphenyl)-prop-2-en-1-one **8a**.** Pale yellow crystals (95%); mp 101–103 °C;  $\delta_{\text{H}}/\text{ppm}$  (300 MHz,  $\text{CDCl}_3$ ) 3.89 (3H, s), 3.96 (3H, s), 3.98 (6H, s), 6.97 (2H, d,  $J$  9.0 Hz), 7.30 (2H, s), 7.41 (1H, d,  $J$  15.6 Hz), 7.65 (2H, d,  $J$  9.0 Hz), 7.84 (1H, d,  $J$  15.1 Hz).

**4.2.1.2. (E)-3-(3-Fluoro-4-methoxyphenyl)-1-(3,4,5-trimethoxyphenyl)prop-2-en-1-one **8b**.** Yellow solid (95%); mp 103–105 °C;  $\delta_{\text{H}}/\text{ppm}$  (300 MHz,  $\text{CDCl}_3$ ) 3.94 (6H, s), 3.96 (6H, s), 6.99 (1H, t,  $J$  8.5 Hz), 7.27 (2H, s), 7.33–7.46 (2H, m), 7.35 (1H,  $J$  15.8 Hz), 7.74 (1H, d,  $J$  15.8 Hz).

**4.2.1.3. (E)-3-(3-Hydroxy-4-methoxyphenyl)-1-(3,4,5-trimethoxyphenyl)prop-2-en-1-one **8c**.** Yellow powder (82%); mp 144–146 °C;  $\delta_{\text{H}}/\text{ppm}$  (300 MHz,  $\text{CDCl}_3$ ) 3.93 (3H, s), 3.95 (9H, s), 5.78 (1H, s), 6.87 (1H, d,  $J$  8.3 Hz), 7.13 (1H, dd,  $J$  2.0, 8.3 Hz), 7.25–7.30 (3H, m), 7.35 (1H, d,  $J$  15.5 Hz), 7.75 (1H, d,  $J$  15.5 Hz).

**4.2.1.4. (E)-3-[3-(tert-Butyl-dimethyl-silyloxy)-4-methoxyphenyl]-1-(3,4,5-trimethoxyphenyl)-prop-2-en-1-one **8d**.** To a solution of chalcone **8c** (1.03 g, 3.0 mmol) in DMF (10 mL), was added diisopropylethylamine (1.44 g, 3.0 mmol) and *tert*-butyl-dimethylsilyl chloride (TBDMS-Cl) (1.36 g, 9.0 mmol). The mixture was heated under reflux for 1 h and cooled down to room temperature. Water (10 mL) was added to the mixture and extracted with DCM ( $3 \times 20$  mL). The combined organic extracts were washed with brine (30 mL), dried over anhydrous magnesium sulfate, filtered and evaporated in vacuo. The resulting yellow solid was purified by flash chromatography ( $\text{SiO}_2$ , ethyl acetate:cyclohexane, 1:1) to afford chalcone **8d** as a pale yellow powder (1.17 g, 85% yield); mp 114–115 °C;  $\delta_{\text{H}}/\text{ppm}$  (400 MHz,  $\text{CDCl}_3$ ) 0.21 (6H, s), 1.04 (9H, s), 3.86 (3H, s), 3.95 (6H, s), 3.96 (3H, s), 6.89 (1H, d,  $J$  8.4 Hz), 7.19 (1H, d,  $J$  2.1 Hz), 7.27 (1H, dd,  $J$  2.1; 8.4 Hz), 7.29 (2H, s), 7.36 (1H, d,  $J$  15.6 Hz), 7.74 (1H, d,  $J$  15.6 Hz);  $\delta_{\text{C}}/\text{ppm}$  (100 MHz,  $\text{CDCl}_3$ ) –4.4 ( $2 \times \text{CH}_3$ ), 18.6 (C), 26.0 ( $3 \times \text{CH}_3$ ), 55.7 ( $\text{CH}_3$ ), 56.5 ( $2 \times \text{CH}_3$ ), 61.1 ( $\text{CH}_3$ ), 106.3 ( $2 \times \text{CH}$ ), 112.1 (CH), 120.0 (CH), 120.6 (CH), 123.7 (CH), 128.3 (C), 134.1 (C), 142.5 (C), 144.8 (CH), 145.5 (C), 153.4 ( $2 \times \text{C}$ ), 153.7 (C), 189.3 (C=O);  $m/z$  (CI) 459 (100%,  $\text{M}+\text{H}^+$ ), 401 (50,  $\text{M}-\text{tBu}$ ).

### 4.2.2. General procedure for $\alpha$ -bromination of chalcones

A standardised solution of bromine in chloroform (17 mL,  $1 \text{ mol L}^{-1}$ ) was added dropwise to the chalcone **8a**, **8b** or **8d** (17 mmol) in chloroform (90 mL) at 0 °C while being vigorously stirred under a nitrogen atmosphere. The solution turns from yellow to red/brown. After 0.5 h at 0 °C, chloroform was removed in vacuo leaving a red solid (2,3-dibrominated). Triethylamine (50 mL) was added slowly to a stirred solution of 2,3-dibromo-chalcone (5 mmol) in chloroform (5 mL) at 0 °C. The mixture was heated under reflux for 1 h and solvents were removed in vacuo. The resulting cream powder was dissolved in chloroform (ca. 30 mL) and washed with water ( $3 \times 20$  mL) and aqueous solution of saturated sodium bicarbonate ( $2 \times 20$  mL). The organic layer was dried over anhydrous  $\text{MgSO}_4$ , filtered, evaporated and recrystallised from ethyl acetate and hexane to afford the  $\alpha$ -bromo-chalcones. (NB: These products are light-sensitive and isomerise readily.)

**4.2.2.1. (Z)-2-Bromo-3-(4-methoxy-phenyl)-1-(3,4,5-trimethoxy-phenyl)-prop-2-en-1-one **10a**.** Yellow solid (44%); mp 113–114 °C;  $\delta_{\text{H}}/\text{ppm}$  (400 MHz,  $\text{CDCl}_3$ ) 3.87 (3H, s), 3.89 (6H, s), 3.94 (3H, s), 6.97 (2H, d,  $J$  8.9 Hz), 7.03 (2H, s), 7.69 (1H, s), 7.91 (2H, d,  $J$  8.9 Hz);  $\delta_{\text{C}}/\text{ppm}$  (100 MHz,  $\text{CDCl}_3$ ) 55.8 ( $\text{CH}_3$ ), 56.8 ( $2 \times \text{CH}_3$ ), 61.4 ( $\text{CH}_3$ ), 107.7 ( $2 \times \text{CH}$ ), 114.4 ( $2 \times \text{CH}$ ), 120.1 (C), 126.4 (C), 132.2 (C), 132.9 ( $2 \times \text{CH}$ ), 142.3 (C), 142.7 (CH), 153.5 ( $2 \times \text{C}$ ), 161.9 (C), 191.2 (C=O);  $m/z$  (CI) 409 (100%,  $\text{M}_{\text{Br}}^{81}+\text{H}^+$ ), 407 (95,  $\text{M}_{\text{Br}}^{79}+\text{H}^+$ ).

**4.2.2.2. (Z)-2-Bromo-3-(3-fluoro-4-methoxy-phenyl)-1-(3,4,5-trimethoxy-phenyl)-prop-2-en-1-one **10b**.** White powder (73%); mp 116–117 °C;  $\delta_{\text{H}}/\text{ppm}$  (400 MHz,  $\text{CDCl}_3$ ) 3.90 (6H, s), 3.94 (6H, s), 7.01 (1H, m), 7.05 (2H, s), 7.56 (1H, d,  $J$  12.6 Hz), 7.63 (1H, s), 7.86 (1H, dd,  $J$  2.0; 12.6 Hz);  $\delta_{\text{C}}/\text{ppm}$  (100 MHz,  $\text{CDCl}_3$ ) 56.6 ( $\text{CH}_3$ ), 56.7 ( $2 \times \text{CH}_3$ ), 61.3 ( $\text{CH}_3$ ), 107.6 ( $2 \times \text{CH}$ ), 113.2 (CH, d,  $J$  1 Hz), 117.7 (CH, d,  $J$  20 Hz), 121.0 (C), 126.7 (C, d,  $J$  7 Hz), 128.4 (CH, d,  $J$  3 Hz), 131.7 (C), 141.0 (CH), 142.5 (C), 149.9 (C, d,  $J$  11 Hz), 152.0 (C, d,  $J$  247 Hz), 153.5 ( $2 \times \text{C}$ ), 190.8 (C=O);  $m/z$  (CI) 427 (98%,  $\text{M}_{\text{Br}}^{81}+\text{H}^+$ ), 425 (100,  $\text{M}_{\text{Br}}^{79}+\text{H}^+$ ).

**4.2.2.3. (Z)-2-Bromo-3-[3-(tert-butyl-dimethyl-silyloxy)-4-methoxy-phenyl]-1-(3,4,5-trimethoxy-phenyl)-prop-2-en-1-one **10c**.** White powder (66%); mp 107–108 °C;  $\delta_{\text{H}}/\text{ppm}$  (400 MHz,  $\text{CDCl}_3$ ) 0.18 (6H, s), 1.00 (9H, s), 3.85 (3H, s), 3.88 (6H, s), 3.93 (3H, s), 6.88 (1H, d,  $J$  8.5 Hz), 7.02 (2H, s), 7.41 (1H, dd,  $J$  2.2; 8.5 Hz), 7.62 (1H, s), 7.64 (1H, d,  $J$  2.2 Hz);  $\delta_{\text{C}}/\text{ppm}$  (100 MHz,  $\text{CDCl}_3$ ) –4.2 ( $2 \times \text{CH}_3$ ), 18.8 (C), 26.1 ( $3 \times \text{CH}_3$ ), 55.9 ( $\text{CH}_3$ ), 56.8 ( $2 \times \text{CH}_3$ ), 61.4 ( $\text{CH}_3$ ), 107.6 ( $2 \times \text{CH}$ ), 111.8 (CH), 120.0 (C), 122.8 (CH), 126.4 (CH), 126.6 (C), 132.2 (C), 142.3 (C), 142.8 (CH), 145.1 (C), 153.3 ( $2 \times \text{C}$ ), 153.7 (C), 191.1 (C=O);  $m/z$  (CI) 539 (95%,  $\text{M}_{\text{Br}}^{81}+\text{H}^+$ ), 537 (100,  $\text{M}_{\text{Br}}^{79}+\text{H}^+$ ), 481 (50,  $\text{M}_{\text{Br}}^{81}-\text{tBu}$ ), 479 (55,  $\text{M}_{\text{Br}}^{79}-\text{tBu}$ ).

### 4.2.3. General procedure for the Suzuki coupling

A mixture of  $\alpha$ -bromo-chalcone **10a–c** (1.0 mmol), substituted phenyl boronic acid **11a–f** (1.2 mmol), tris(dibenzylideneaceton)dipalladium(0) (23 mg, 0.022 mmol) and triphenylphosphine (11 mg, 0.042 mmol) was dissolved in toluene (6 mL) and *n*-PrOH (2 mL) and degassed. After stirring for 10 min, diethylamine (0.13 mL, 1.3 mmol) and  $\text{H}_2\text{O}$  (1.6 mL) were added. The mixture was degassed a second time, heated under reflux for 1 h, then cooled down to room temperature and poured into ethyl acetate (100 mL). The aqueous layer was separated, and the remaining organic layer was washed with 0.2 M NaOH (30 mL), 0.05 M HCl (30 mL) and  $\text{H}_2\text{O}$  (30 mL), dried over anhydrous  $\text{MgSO}_4$ , and filtered. The solvent was removed in vacuo, and the product was purified by column chromatography ( $\text{SiO}_2$ , ethyl acetate/hexane 1:3) and recrystallised from ethyl acetate/hexane to afford the  $\alpha$ -

aryl-chalcones **12a–h**. Chalcones **12** were obtained exclusively as *E*-isomers as ascertained by  $^1\text{H}$  NMR and X-ray crystallography. The samples were stored away from the light to avoid isomerisation.

**4.2.3.1. (E)-2-(2-Hydroxy-phenyl)-3-(4-methoxy-phenyl)-1-(3,4,5-trimethoxy-phenyl)-prop-2-en-1-one 12a.** Yellow solid (48%); mp 69–70 °C;  $\delta_{\text{H}}/\text{ppm}$  (400 MHz,  $\text{CDCl}_3$ ) 3.67 (3H, s), 3.79 (6H, s), 3.85 (3H, s), 6.62 (2H, d, *J* 8.8 Hz), 6.78 (1H, ddd, *J* 0.9; 7.5; 7.5 Hz), 6.94 (2H, d, *J* 8.8 Hz), 6.97 (1H, dd, *J* 0.9; 7.5 Hz), 7.01 (1H, m), 7.12 (2H, s), 7.14 (1H, s), 7.18 (1H, m);  $\delta_{\text{C}}/\text{ppm}$  (100 MHz,  $\text{CDCl}_3$ ) 55.6 ( $\text{CH}_3$ ), 56.7 ( $2 \times \text{CH}_3$ ), 61.3 ( $\text{CH}_3$ ), 108.2 ( $2 \times \text{CH}$ ), 114.3 ( $2 \times \text{CH}$ ), 118.5 (CH), 121.3 (CH), 124.3 (C), 127.1 (C), 130.6 (CH), 131.1 (CH), 132.3 (C), 132.4 ( $2 \times \text{CH}$ ), 135.4 (C), 141.4 (CH), 153.3 ( $2 \times \text{C}$ ), 153.3 (C), 155.0 (C), 160.9 (C), 199.3 (C=O);  $\nu_{\text{max}}$  (KBr) 3416 (OH), 1582 (C=O); *m/z* (CI) 421 (40,  $\text{M}+\text{H}^+$ ), 128 (100); HRMS found  $[\text{MH}]^+$  421.1649,  $\text{C}_{25}\text{H}_{24}\text{O}_6$  requires  $[\text{MH}]^+$  421.1646.

**4.2.3.2. (E)-3-(3-Fluoro-4-methoxy-phenyl)-2-(2-hydroxy-phenyl)-1-(3,4,5-trimethoxy-phenyl)-prop-2-en-1-one 12b.** Yellow powder (61%); mp 96–97 °C;  $\delta_{\text{H}}/\text{ppm}$  (400 MHz,  $\text{CDCl}_3$ ) 3.84 (3H, s), 3.88 (6H, s), 3.95 (3H, s), 6.75–6.82 (2H, m), 6.89 (1H, m), 6.90 (1H, m), 6.97 (1H, m), 7.11 (1H, m), 7.13 (1H, s), 7.24 (2H, s), 7.29 (1H, m);  $\delta_{\text{C}}/\text{ppm}$  (100 MHz,  $\text{CDCl}_3$ ) 56.5 ( $\text{CH}_3$ ), 56.7 ( $2 \times \text{CH}_3$ ), 61.4 ( $\text{CH}_3$ ), 108.2 ( $2 \times \text{CH}$ ), 113.1 (CH), 117.6 (d, CH, *J* 19 Hz), 118.6 (CH), 121.5 (CH), 123.7 (C), 127.6 (d, C, *J* 9 Hz), 127.7 (CH), 130.8 (CH), 130.9 (CH), 131.8 (C), 136.7 (C), 139.6 (CH), 143.2 (C), 149.0 (d, C, *J* 11 Hz), 152.2 (d, C, *J* 251 Hz), 153.3 ( $2 \times \text{C}$ ), 154.9 (C), 200.2 (C=O);  $\nu_{\text{max}}$  (KBr) 3417 (OH), 1581 (C=O); *m/z* (EI) 438 (10%,  $\text{M}^+$ ), 195 (100); HRMS found  $[\text{MH}]^+$  439.1554,  $\text{C}_{25}\text{H}_{24}\text{O}_6\text{F}$  requires  $[\text{MH}]^+$  439.1551.

**4.2.3.3. (E)-3-[3-(tert-Butyl-dimethyl-silyloxy)-4-methoxy-phenyl]-2-(2-hydroxy-phenyl)-1-(3,4,5-trimethoxy-phenyl)-prop-2-en-1-one 12c.** Yellow powder (84%); mp 122–123 °C;  $\delta_{\text{H}}/\text{ppm}$  (400 MHz,  $\text{CDCl}_3$ ) 0.01 (6H, s), 0.90 (9H, s), 3.78 (3H, s), 3.90 (6H, s), 3.96 (3H, s), 6.56 (1H, d, *J* 1.9 Hz), 6.70 (1H, d, *J* 8.5 Hz), 6.76 (1H, dd, *J* 1.9; 8.5 Hz), 6.89 (1H, dd, *J* 7.3; 7.6 Hz), 7.07 (1H, d, *J* 7.9 Hz), 7.12 (1H, dd, *J* 1.3; 7.6 Hz), 7.14 (1H, s), 7.24 (2H, s), 7.28 (1H, ddd, *J* 1.3; 7.3; 7.9 Hz), 7.99 (1H, br s);  $\delta_{\text{C}}/\text{ppm}$  (100 MHz,  $\text{CDCl}_3$ ) –4.4 ( $2 \times \text{CH}_3$ ), 18.7 (C), 26.0 ( $3 \times \text{CH}_3$ ), 55.7 ( $\text{CH}_3$ ), 56.6 ( $2 \times \text{CH}_3$ ), 61.3 ( $\text{CH}_3$ ), 108.1 ( $2 \times \text{CH}$ ), 111.7 (CH), 118.4 (CH), 121.3 (CH), 122.3 (CH), 124.3 (C), 126.1 (CH), 127.4 (C), 130.6 (CH), 131.1 (CH), 132.4 (C), 135.2 (C), 141.4 (CH), 142.8 (C), 145.0 (C), 152.8 (C), 153.2 ( $2 \times \text{C}$ ), 154.9 (C), 199.1 (C=O); *m/z* (EI) 550 (10%,  $\text{M}^+$ ), 493 (40,  $\text{M}-\text{tBu}$ ), 195 (100), HRMS found  $[\text{MH}]^+$  551.2466,  $\text{C}_{25}\text{H}_{25}\text{O}_7$  requires  $[\text{MH}]^+$  551.2460.

**4.2.3.4. (E)-1-(3,4,5-Trimethoxyphenyl)-3-(4-methoxyphenyl)-2-phenylprop-2-en-1-one 12d.** Creamy-coloured fine needles (43%); mp 136–137 °C;  $\delta_{\text{H}}/\text{ppm}$  (400 MHz,  $\text{CDCl}_3$ ) 3.70 (3H, s), 3.75 (6H, s), 3.83 (3H, s), 6.65 (2H, d, *J* 8.8 Hz), 6.98 (2H, s), 6.99 (2H, d, *J* 8.8 Hz), 7.19–7.31 (6H, m);  $\delta_{\text{C}}/\text{ppm}$  (100 MHz,  $\text{CDCl}_3$ ) 55.28 ( $\text{CH}_3$ ), 56.21 ( $2 \times \text{CH}_3$ ), 60.97 ( $\text{CH}_3$ ), 107.31 ( $2 \times \text{CH}$ ), 113.77 ( $2 \times \text{CH}$ ), 127.33 (C), 127.86 ( $2 \times \text{CH}$ ), 128.98 (CH), 129.74 ( $2 \times \text{CH}$ ), 132.22 ( $2 \times \text{CH}$ ), 133.31 (C), 137.33 (C), 138.58 (C), 140.02 (CH), 141.37 (C), 152.71 (C), 160.27 (C), 196.17 (C=O); *m/z* (AP+) 405 ( $\text{MH}^+$ , 100), HRMS found  $[\text{MH}]^+$  405.1697,  $\text{C}_{25}\text{H}_{25}\text{O}_5$  requires  $[\text{MH}]^+$  405.1697.

**4.2.3.5. (E)-1-(3,4,5-Trimethoxyphenyl)-2,3-bis(4-methoxy-phenyl)prop-2-en-1-one 12e.** Yellow solid (30%); mp 112–114 °C;  $\delta_{\text{H}}/\text{ppm}$  (400 MHz,  $\text{CDCl}_3$ ) 3.71 (3H, s), 3.75 (6H, s), 3.76 (3H, s), 3.83 (3H, s), 6.66 (2H, d, *J* 8.8 Hz), 6.83 (2H, d, *J* 8.7 Hz), 6.98 (2H, s), 7.03 (2H, d, *J* 8.8 Hz), 7.13 (2H, d, *J* 8.7 Hz), 7.16 (H,

s);  $\delta_{\text{C}}/\text{ppm}$  (100 MHz,  $\text{CDCl}_3$ ) 55.27 ( $\text{CH}_3$ ), 55.28 ( $\text{CH}_3$ ), 56.21 ( $2 \times \text{CH}_3$ ), 60.96 ( $\text{CH}_3$ ), 107.29 ( $2 \times \text{CH}$ ), 113.76 ( $2 \times \text{CH}$ ), 114.40 ( $2 \times \text{CH}$ ), 127.56 (C), 129.40 (C), 130.95 ( $2 \times \text{CH}$ ), 132.11 ( $2 \times \text{CH}$ ), 133.40 (C), 138.26 (C), 139.43 (CH), 141.32 (C), 152.70 (C), 159.19 (C), 160.14 (C), 196.61 (C=O); *m/z* (AP+) 435 ( $\text{MH}^+$ , 100); HRMS found  $[\text{MH}]^+$  435.1799,  $\text{C}_{26}\text{H}_{27}\text{O}_6$  requires  $[\text{MH}]^+$  435.1802.

**4.2.3.6. (E)-2-(2,4-Dimethoxyphenyl)-1-(3,4,5-trimethoxy-phenyl)-3-(4-methoxyphenyl)prop-2-en-1-one 12f.** Cream crystals (37%); mp 124–126 °C;  $\delta_{\text{H}}/\text{ppm}$  (400 MHz,  $\text{CDCl}_3$ ) 3.59 (3H, s), 3.78 (3H, s), 3.81 (6H, s), 3.83 (3H, s), 3.89 (3H, s), 6.44–6.51 (2H, m), 6.73 (2H, d, *J* 8.6 Hz), 7.07 (2H, s), 7.10 (1H, d, *J* 8.0 Hz), 7.14 (2H, d, *J* 8.6 Hz), 7.23 (H, s);  $\delta_{\text{C}}/\text{ppm}$  (100 MHz,  $\text{CDCl}_3$ ) 55.25 ( $\text{CH}_3$ ), 55.39 ( $\text{CH}_3$ ), 55.49 ( $\text{CH}_3$ ), 56.15 ( $2 \times \text{CH}_3$ ), 60.93 ( $\text{CH}_3$ ), 99.07 (CH), 105.23 (CH), 106.96 ( $2 \times \text{CH}$ ), 113.63 ( $2 \times \text{CH}$ ), 119.44 (C), 128.04 (C), 131.69 (CH), 131.75 ( $2 \times \text{CH}$ ), 133.87 (C), 135.42 (C), 139.68 (CH), 141.00 (C), 152.52 (C), 158.05 (C), 159.98 (C), 161.08 (C), 197.09 (C=O); *m/z* (AP+) 465 ( $\text{MH}^+$ , 100); HRMS found  $[\text{MH}]^+$  465.1901,  $\text{C}_{27}\text{H}_{29}\text{O}_7$  requires  $[\text{MH}]^+$  465.1908.

**4.2.3.7. (E)-2-(4-(Dimethylamino)phenyl)-1-(3,4,5-trimethoxy-phenyl)-3-(4-methoxyphenyl)prop-2-en-1-one 12g.** Yellow crystals (26%); mp 129–131 °C;  $\delta_{\text{H}}/\text{ppm}$  (400 MHz,  $\text{CDCl}_3$ ) 2.97 (6H, s), 3.78 (3H, s), 3.80 (6H, s), 3.89 (3H, s), 6.68 (2H, d, *J* 8.8 Hz), 6.74 (2H, d, *J* 8.8 Hz), 7.07 (2H, s), 7.10–7.14 (3H, m), 7.18 (2H, d, *J* 8.8 Hz);  $\delta_{\text{C}}/\text{ppm}$  (100 MHz,  $\text{CDCl}_3$ ) 40.79 ( $2 \times \text{CH}_3$ ), 55.62 ( $\text{CH}_3$ ), 56.55 ( $2 \times \text{CH}_3$ ), 61.30 ( $\text{CH}_3$ ), 107.76 ( $2 \times \text{CH}$ ), 112.97 ( $2 \times \text{CH}$ ), 114.04 ( $2 \times \text{CH}$ ), 125.07 (C), 128.52 (C), 130.89 ( $2 \times \text{CH}$ ), 132.32 ( $2 \times \text{CH}$ ), 133.82 (C), 137.82 (CH), 139.41 (C), 150.32 (C), 152.98 (C), 153.43 (C–N), 160.19 (C), 197.36 (C=O); *m/z* (AP+) 448 ( $\text{MH}^+$ , 30), 447 (M, 100); HRMS found  $[\text{MH}]^+$  448.2112,  $\text{C}_{27}\text{H}_{30}\text{NO}_5$  requires  $[\text{MH}]^+$  448.2118.

**4.2.3.8. (E)-2-(2,3,4-Trimethoxyphenyl)-1-(3,4,5-trimethoxy-phenyl)-3-(4-methoxyphenyl)prop-2-en-1-one 12h.** Brown oil (61%);  $\delta_{\text{H}}/\text{ppm}$  (400 MHz,  $\text{CDCl}_3$ ) 3.63 (3H, s), 3.71 (3H, s), 3.78 (6H, s), 3.78 (3H, s), 3.82 (3H, s), 3.84 (3H, s), 6.59 (H, d, *J* 8.6 Hz), 6.67 (2H, d, *J* 8.9 Hz), 6.82 (H, d, *J* 8.6 Hz), 7.04 (2H, d, *J* 8.9 Hz), 7.05 (2H, s), 7.15 (H, s);  $\delta_{\text{C}}/\text{ppm}$  (100 MHz,  $\text{CDCl}_3$ ) 55.26 ( $\text{CH}_3$ ), 55.98 ( $\text{CH}_3$ ), 56.21 ( $2 \times \text{CH}_3$ ), 60.69 ( $\text{CH}_3$ ), 60.91 ( $\text{CH}_3$ ), 60.93 ( $\text{CH}_3$ ), 107.15 (CH), 107.61 ( $2 \times \text{CH}$ ), 113.61 ( $2 \times \text{CH}$ ), 124.43 (C), 125.45 (CH), 127.56 (C), 131.86 ( $2 \times \text{CH}$ ), 133.82 (C), 135.38 (C), 140.39 (CH), 141.20 (C), 142.42 (C), 151.45 (C), 152.64 (C), 153.94 (C), 160.17 (C), 197.07 (C=O); *m/z* (AP+) 495 ( $\text{MH}^+$ , 50), 117 (100); HRMS found  $[\text{MH}]^+$  495.2008,  $\text{C}_{19}\text{H}_{18}\text{O}_6$  requires  $[\text{MH}]^+$  495.2013.

**4.2.3.9. (E)-3-(3-Hydroxy-4-methoxy-phenyl)-2-(2-hydroxy-phenyl)-1-(3,4,5-trimethoxy-phenyl)-prop-2-en-1-one 12i.** To a solution of **12c** (0.56 mmol) in dry THF (10 mL) was added a 1 M solution of TBAF in THF (2 mmol). The yellow solution turned red and was left to stir for 30 min, then neutralised with water (20 mL). The aqueous solution was extracted with DCM ( $3 \times 20$  mL) and the combined organic layers were washed with water (20 mL) then brine (20 mL). The organic extract was dried over anhydrous  $\text{MgSO}_4$ , filtered and evaporated in vacuo. Purification by flash chromatography ( $\text{SiO}_2$ , ethyl acetate:cyclohexane, 1:3) afforded chalcone **12i** as a yellow foamy solid (95%); mp 87–88 °C;  $\delta_{\text{H}}/\text{ppm}$  (400 MHz,  $\text{CDCl}_3$ ) 3.75 (3H, s), 3.80 (6H, s), 3.86 (3H, s), 6.53–6.59 (2H, m), 6.55 (1H, s), 6.79 (1H, ddd, *J* 1.1; 7.5; 7.6 Hz), 6.97 (1H, d, *J* 8.0 Hz), 7.03 (1H, d, *J* 7.6 Hz), 7.06 (1H, s), 7.15 (2H, s), 7.18 (1H, ddd, *J* 1.8; 7.5; 8.0 Hz);  $\delta_{\text{C}}/\text{ppm}$  (100 MHz,  $\text{CDCl}_3$ ) 56.2 ( $\text{CH}_3$ ), 56.7 ( $2 \times \text{CH}_3$ ), 61.4 ( $\text{CH}_3$ ), 108.2 ( $2 \times \text{CH}$ ), 110.7 (CH), 116.5 (CH), 118.6 (CH), 121.3 (CH), 123.9 (CH), 124.1 (C), 127.9 (C), 130.7 (CH), 131.0 (CH), 132.0 (C), 135.8 (C), 141.2 (CH), 143.1 (C), 145.7

(C), 148.2 (C), 153.3 (2 × C), 154.9 (C), 199.3 (C=O);  $\nu_{\max}$  (KBr) 3415 (OH), 1582 (C=O);  $m/z$  (EI) 434 (60%, M<sup>+</sup>), 195 (100); HRMS found [MH]<sup>+</sup> 437.1590, C<sub>25</sub>H<sub>24</sub>O<sub>7</sub> requires [MH]<sup>+</sup> 495.1595.

#### 4.2.4. General procedure for the preparation of alcohols 16a–c

The substituted benzyl halide **15a–c** (38 mmol) was added to a mixture of magnesium turnings (38 mmol) and one crystal of iodine in anhydrous diethyl ether (40 mL) and stirred under reflux for 30 min. The resulting grey solution was cooled to –78 °C and a solution of 3,4,5-trimethoxybenzaldehyde **9f** (5 g, 25.5 mmol) in anhydrous THF (10 mL) was added over 10 min. The reaction was allowed to warm to 0 °C and subsequently poured into a separating funnel containing 1 N HCl (10 mL) and ice (10 g). The product was extracted into ethyl acetate (3 × 20 mL) and the organic phases dried over MgSO<sub>4</sub>. Removal of the solvent by rotary evaporation afforded the crude product which was subjected to column chromatography over silica gel. Further purification of the resulting solid by recrystallisation afforded the alcohol in good yields (68–91%).

2-Phenyl-1-(3,4,5-trimethoxyphenyl)ethanol **16a** as white crystals (68%). Mp: 83–84 °C;  $\delta_{\text{H}}$ /ppm (400 MHz, CDCl<sub>3</sub>) 2.97–3.00 (2H, m), 3.83 (6H, s), 3.83 (3H, s), 4.81 (1H, dd, *J* 5.6; 7.5 Hz), 6.54 (2H, s), 7.18–7.32 (5H, m);  $\delta_{\text{C}}$ /ppm (100 MHz, CDCl<sub>3</sub>) 46.3, 56.3, 61.1, 75.7, 103.0, 126.9, 128.7, 129.8, 137.4, 138.2, 139.8, 153.4; MS (ES<sup>+</sup>) 289.1 (30%, [M+H]<sup>+</sup>), 271.1 (100%, [M–H<sub>2</sub>O]<sup>+</sup>).

2-(4-Methoxyphenyl)-1-(3,4,5-trimethoxyphenyl)ethanol **16c** as white crystals (75%). Mp: 120–121 °C;  $\delta_{\text{H}}$ /ppm (400 MHz, CDCl<sub>3</sub>) 2.05 (1H, br s), 2.87–2.98 (2H, m), 3.79 (3H, s), 3.84 (9H, s), 4.77 (1H, dd, *J* 5.0; 8.0 Hz), 6.55 (2H, s), 6.85 (2H, d, *J* 8.5 Hz), 7.11 (2H, d, *J* 8.5 Hz);  $\delta_{\text{C}}$ /ppm (100 MHz, CDCl<sub>3</sub>) 45.4, 55.5, 56.3, 61.1, 75.8, 103.0, 114.1, 130.1, 130.7, 137.4, 139.9, 153.4, 158.6; MS (ES<sup>+</sup>) 319.1 (20%, [M+H]<sup>+</sup>), 301.1 (100%, [M–H<sub>2</sub>O]<sup>+</sup>).

#### 4.2.5. General procedure for the preparation of ketones 14a–c

Pyridinium chlorochromate (11 mmol) was suspended in anhydrous DCM (10 mL) and a solution of alcohol **16a–c** (7.3 mmol) in DCM (10 mL) was rapidly added at ambient temperature. The solution became briefly homogeneous before depositing the reduced reagent as a black insoluble solid around the walls of the reaction flask. The reaction was stirred at room temperature and monitored for completion by TLC (3–5 h). The black reaction mixture was diluted with DCM and filtered through Celite. The Celite was washed several times with DCM and the filtrate concentrated under reduced pressure. The product was purified by column chromatography over silica gel and the resulting solid recrystallised to afford ketones **14a–c** in good yields (76–80%).

##### 4.2.5.1. 2-Phenyl-1-(3,4,5-trimethoxyphenyl)ethanone

**14a**. Colourless crystals (78%). Mp: 95–96 °C;  $\delta_{\text{H}}$ /ppm (400 MHz, CDCl<sub>3</sub>) 3.88 (6H, s), 3.90 (3H, s), 4.25 (2H, s), 7.21–7.38 (7H, m);  $\delta_{\text{C}}$ /ppm (100 MHz, CDCl<sub>3</sub>) 45.9, 56.5, 61.2, 106.5, 127.2, 129.0, 129.5, 131.9, 135.1, 142.8, 153.2, 196.7; MS (ES<sup>+</sup>) 287.1 (100%, [M+H]<sup>+</sup>); HRMS found [MH]<sup>+</sup> 287.1285, C<sub>17</sub>H<sub>18</sub>O<sub>4</sub> requires [MH]<sup>+</sup> 287.1278.

##### 4.2.5.2. 2-*p*-Tolyl-1-(3,4,5-trimethoxyphenyl)ethanone

**14b**. Pale yellow powder (80%). Mp: 73–74 °C;  $\delta_{\text{H}}$ /ppm (400 MHz, CDCl<sub>3</sub>) 2.30 (3H, s), 3.86 (6H, s), 3.88 (3H, s), 4.19 (2H, s), 7.10 (4H, m), 7.25 (2H, s);  $\delta_{\text{C}}$ /ppm (100 MHz, CDCl<sub>3</sub>) 21.3, 45.5, 56.4, 61.1, 106.5, 129.3, 129.7, 131.9, 136.7, 142.7, 153.2, 153.9, 196.8; MS (ES<sup>+</sup>) 301.1 (100%, [M+H]<sup>+</sup>); HRMS found [MH]<sup>+</sup> 301.1443, C<sub>18</sub>H<sub>20</sub>O<sub>4</sub> requires [MH]<sup>+</sup> 301.1434.

**4.2.5.3. 2-(4-Methoxyphenyl)-1-(3,4,5-trimethoxyphenyl)ethanone 14c**. Pale yellow powder (76%). Mp: 81–82 °C;  $\delta_{\text{H}}$ /ppm (400 MHz, CDCl<sub>3</sub>) 3.76 (3H, s), 3.87 (6H, s), 3.89 (3H, s), 4.17 (2H,

s), 6.85 (2H, d, *J* 8.6 Hz), 7.17 (2H, d, *J* 8.6 Hz), 7.24 (2H, s);  $\delta_{\text{C}}$ /ppm (100 MHz, CDCl<sub>3</sub>) 44.9, 55.4, 56.4, 61.1, 106.4, 114.4, 127.0, 130.5, 131.9, 142.7, 153.2, 158.8, 196.9; MS (ES<sup>+</sup>) 317.1 (100%, [M+H]<sup>+</sup>); HRMS found [MH]<sup>+</sup> 317.1384, C<sub>18</sub>H<sub>20</sub>O<sub>5</sub> requires [MH]<sup>+</sup> 317.1384.

#### 4.2.6. General procedure for the preparation of alpha-aryl chalcones 13

A mixture of ketone **14a–c** (0.7 mmol) and the appropriate benzaldehyde **9a–e** (0.7 mmol) in anhydrous benzene (2 mL) was treated at room temperature with piperidine (5  $\mu$ L). The reaction was brought to reflux and water removed by passing the vapours through a condenser packed with molecular sieves (4 Å, held in place with glass wool). The reaction was followed by TLC for completion (6–8 h). On completion, the reaction mixture was poured into water and the phases separated. The aqueous phase was extracted with ethyl acetate (3 × 20 mL) and the combined organic phases dried over MgSO<sub>4</sub>. After filtration and evaporation of the solvent in vacuo, the crude product was purified by column chromatography. Chalcones **13** were obtained as mixtures of *E*- and *Z*-isomers. The ratio of each isomer was determined by NMR (<sup>1</sup>H and HMBC and NOE) and X-ray crystallography. The samples were stored away from the light to avoid isomerisation.

**4.2.6.1. 3-(4-Methoxyphenyl)-2-phenyl-1-(3,4,5-trimethoxyphenyl)prop-2-en-1-one 13a**. Yellow oil which solidified on standing (91%, two isomers, ratio 10:17);  $\delta_{\text{H}}$ /ppm (400 MHz, CDCl<sub>3</sub>) 3.61 (isomer 2, 3H, s), 3.63 (isomer 1, 3H, s), 3.67 (isomer 2, 6H, s), 3.70 (isomer 1, 6H, s), 3.77 (isomer 2, 3H, s), 3.80 (isomer 1, 3H, s), 6.59–6.61 (isomer 1, 2H, m), 6.62–6.65 (isomer 2, 2H, m), 6.97 (isomer 2, 2H, s), 7.04 (isomer 1, 2H, s), 7.13–7.34 (isomer 1, 8H, m; isomer 2, 8H, m); MS (ES<sup>+</sup>) 405.1 (100%, [M+H]<sup>+</sup>); HRMS found [MH]<sup>+</sup> 405.1706, C<sub>25</sub>H<sub>24</sub>O<sub>5</sub> requires [MH]<sup>+</sup> 405.1697.

**4.2.6.2. 3-(3-Hydroxy-4-methoxyphenyl)-2-phenyl-1-(3,4,5-trimethoxyphenyl)prop-2-en-1-one 13b**. Yellow oil which solidified on standing, further purified by recrystallisation from hexane/ethyl acetate (74%, single isomer);  $\delta_{\text{H}}$ /ppm (400 MHz, CDCl<sub>3</sub>) 3.82 (6H, s), 3.86 (3H, s), 3.90 (3H, s), 5.46 (1H, s), 6.67 (1H, s), 6.68 (2H, s), 7.06 (2H, s), 7.23–7.39 (6H, m); MS (ES<sup>+</sup>) 421 (100%, [M+H]<sup>+</sup>); HRMS found [MH]<sup>+</sup> 421.1649, C<sub>25</sub>H<sub>24</sub>O<sub>6</sub> requires [MH]<sup>+</sup> 421.1646.

**4.2.6.3. 2,3-diphenyl-1-(3,4,5-trimethoxyphenyl)prop-2-en-1-one 13c**. Sticky yellow oil which partially solidified on standing (80%, two isomers, ratio 10:14);  $\delta_{\text{H}}$ /ppm (400 MHz, CDCl<sub>3</sub>) 3.77 (isomer 2, 6H, s), 3.81 (isomer 1, 6H, s), 3.86 (isomer 2, 3H, s), 3.90 (isomer 1, 3H, s), 7.12–7.37 (isomer 1, 12H, m; isomer 2, 12H, m), 7.44–7.47 (isomer 1, 1H, m; isomer 2, 1H, m); MS (ES<sup>+</sup>) 375.1 (100%, [M+H]<sup>+</sup>); HRMS found [MH]<sup>+</sup> 375.1597, C<sub>24</sub>H<sub>22</sub>O<sub>4</sub> requires [MH]<sup>+</sup> 375.1591.

**4.2.6.4. 3-(4-Methoxy-3-nitrophenyl)-2-phenyl-1-(3,4,5-trimethoxyphenyl)prop-2-en-1-one 13d**. Thick yellow oil (90%, two isomers, ratio 1:2);  $\delta_{\text{H}}$ /ppm (400 MHz, CDCl<sub>3</sub>) 3.79 (isomer 2, 6H, s), 3.80 (isomer 1, 6H, s), 3.88 (isomer 2, 3H, d, *J* 0.8 Hz), 3.90 (isomer 1, 3H, s; isomer 2, 3H, s), 3.91 (isomer 1, 3H, s), 6.88 (isomer 1, 1H, d, *J* 8.8 Hz), 6.92 (isomer 2, 1H, d, *J* 8.8 Hz), 7.06–7.47 (isomer 1, 9H, m; isomer 2, 9H, m), 7.61 (isomer 1, 1H, d, *J* 2.0 Hz), 7.81 (isomer 2, 1H, d, *J* 2.4 Hz); MS (ES<sup>+</sup>) 450.1 (100%, [M+H]<sup>+</sup>); HRMS found [MH]<sup>+</sup> 450.1553, C<sub>25</sub>H<sub>23</sub>NO<sub>7</sub> requires [MH]<sup>+</sup> 450.1547.

**4.2.6.5. 3-(3-fluoro-4-methoxyphenyl)-2-phenyl-1-(3,4,5-trimethoxyphenyl)prop-2-en-1-one 13e**. Thick yellow oil (87%, two isomers, ratio 2:3);  $\delta_{\text{H}}$ /ppm (400 MHz, CDCl<sub>3</sub>) 3.79 (isomer 2, 6H, s), 3.81 (isomer 1, 6H, s), 3.84 (isomer 2, 3H, s), 3.86 (isomer

1, 3H, s), 3.89 (isomer 2, 3H, d, *J* 0.4 Hz), 3.90 (isomer 1, 3H, d, *J* 0.4 Hz), 6.76–7.43 (isomer 1, 11H, m; isomer 2, 11H, m); MS ( $\text{ES}^+$ ) 423.1 (100%,  $[\text{M}+\text{H}]^+$ ); HRMS found  $[\text{MH}]^+$  423.1610,  $\text{C}_{25}\text{H}_{23}\text{FO}_5$  requires  $[\text{MH}]^+$  423.1602.

**4.2.6.6. 3-Phenyl-2-*p*-tolyl-1-(3,4,5-trimethoxyphenyl)prop-2-en-1-one 13f.** Thick yellow oil (93%, two isomers, ratio ~2:1);  $\delta_{\text{H}}/\text{ppm}$  (400 MHz,  $\text{CDCl}_3$ ) 2.34 (isomer 1, 3H, s), 2.35 (isomer 2, 3H, s), 3.77 (isomer 1, 6H, s), 3.81 (isomer 1, 3H, s), 3.86 (isomer 2, 6H, s), 3.90 (isomer 2, 3H, s), 7.11–7.35 (isomer 1, 12H, m; isomer 2, 12H, m); MS ( $\text{ES}^+$ ) 389.1 (100%,  $[\text{M}+\text{H}]^+$ ); HRMS found  $[\text{MH}]^+$  389.1749,  $\text{C}_{25}\text{H}_{24}\text{O}_4$  requires  $[\text{MH}]^+$  389.1747.

**4.2.6.7. 3-(4-Methoxyphenyl)-2-*p*-tolyl-1-(3,4,5-trimethoxyphenyl)prop-2-en-1-one 13g.** Thick yellow oil (77%, two isomers, ratio ~2:1);  $\delta_{\text{H}}/\text{ppm}$  (400 MHz,  $\text{CDCl}_3$ ) 2.33 (3H, s, isomer 1), 2.36 (3H, s, isomer 2), 3.73 (6H, s, isomer 2), 3.76 (3H, s, isomer 2), 3.78 (6H, s, isomer 1), 3.81 (3H, s, isomer 1), 3.87 (3H, s, isomer 1), 3.90 (3H, s, isomer 2), 6.71–6.74 (2H, m, isomer 2), 6.73 (2H, d, *J* 7.6 Hz, isomer 1), 7.06–7.33 (9H, m, isomer 1; 9H, m, isomer 2); MS ( $\text{ES}^+$ ) 419.2 (100%,  $[\text{M}+\text{H}]^+$ ); HRMS found  $[\text{MH}]^+$  419.1858,  $\text{C}_{26}\text{H}_{26}\text{O}_5$  requires  $[\text{MH}]^+$  419.1853.

**4.2.6.8. 3-(3-Hydroxy-4-methoxyphenyl)-2-*p*-tolyl-1-(3,4,5-trimethoxyphenyl)prop-2-en-1-one 13h.** Thick yellow oil (138 mg, 95%);  $\delta_{\text{H}}/\text{ppm}$  (400 MHz,  $\text{CDCl}_3$ ) 2.34 (3H, s, isomer 1), 2.36 (3H, s, isomer 2), 3.76 (6H, s, isomer 2), 3.76 (3H, s, isomer 2), 3.79 (6H, s, isomer 1), 3.81 (3H, s, isomer 1), 3.87 (3H, s, isomer 1), 3.91 (3H, s, isomer 2), 6.71–6.74 (4H, m, isomers 1 and 2), 7.05–7.35 (8H, m, isomer 1; 8H, m, isomer 2); MS ( $\text{ES}^+$ ) 435.1 (100%,  $[\text{M}+\text{H}]^+$ ); HRMS found  $[\text{MH}]^+$  435.1805,  $\text{C}_{26}\text{H}_{26}\text{O}_6$  requires  $[\text{MH}]^+$  435.1802.

**4.2.6.9. 3-(4-Methoxy-3-nitrophenyl)-2-*p*-tolyl-1-(3,4,5-trimethoxyphenyl)prop-2-en-1-one 13i.** Thick yellow oil (58%, two isomers, ratio 6:7);  $\delta_{\text{H}}/\text{ppm}$  (400 MHz,  $\text{CDCl}_3$ ) 2.33 (isomer 2, 3H, s), 2.35 (isomer 1, 3H, s), 3.78 and 3.79 (isomer 1, 6H, s; isomer 2, 6H, s), 3.87 (isomer 2, 3H, d, *J* 1.2 Hz), 3.88 (isomer 1, 3H, s; isomer 2, 3H, s), 3.90 (isomer 1, 3H, s), 6.87–7.45 (isomer 1, 9H, m, H-3; isomer 2, 9H, m), 7.63 (isomer 1, 1H, br s), 7.78 (isomer 2, 1H, br s); MS ( $\text{ES}^+$ ) 464.1 (100%,  $[\text{M}+\text{H}]^+$ ); HRMS found  $[\text{MH}]^+$  464.1711,  $\text{C}_{26}\text{H}_{25}\text{NO}_7$  requires  $[\text{MH}]^+$  464.1704.

**4.2.6.10. 3-(3-Fluoro-4-methoxyphenyl)-2-*p*-tolyl-1-(3,4,5-trimethoxyphenyl)prop-2-en-1-one 13j.** Thick yellow oil (72%, two isomers, ratio 4:11);  $\delta_{\text{H}}/\text{ppm}$  (400 MHz,  $\text{CDCl}_3$ ) 2.34 (isomer 2, 3H, s), 2.37 (isomer 1, 3H, s), 3.79 (isomer 2, 6H, s), 3.81 (isomer 1, 6H, s), 3.82 (isomer 2, 3H, s), 3.85 (isomer 1, 3H, s), 3.88 (isomer 2, 3H, s), 3.92 (isomer 1, 3H, s), 6.76–7.32 (isomer 1, 10H, m; isomer 2, 10H, m); MS ( $\text{ES}^+$ ) 437.1 (100%,  $[\text{M}+\text{H}]^+$ ); HRMS found  $[\text{MH}]^+$  437.1769,  $\text{C}_{26}\text{H}_{25}\text{FO}_5$  requires  $[\text{MH}]^+$  437.1759.

**4.2.6.11. 2-(4-methoxyphenyl)-3-phenyl-1-(3,4,5-trimethoxyphenyl)prop-2-en-1-one 13k.** Thick yellow oil (97%, two isomers, ratio 1:1);  $\delta_{\text{H}}/\text{ppm}$  (400 MHz,  $\text{CDCl}_3$ ) 3.78 (6H, s, isomer 1 or 2), 3.79 (3H, s, isomer 1 or 2), 3.80 (3H, s, isomer 1 or 2), 3.82 (6H, s, isomer 1 or 2), 3.86 (3H, s, isomer 1 or 2), 3.90 (3H, s, isomer 1 or 2), 6.86 (2H, d, *J* 8.8 Hz, isomer 1 or 2), 6.88 (2H, d, *J* 8.4 Hz, isomer 1 or 2), 7.10 (3H, s, isomer 1 or 2), 7.15–7.22 (11H, m, isomer 1 and 2), 7.27–7.29 (4H, m, isomer 1 or 2), 7.37 (1H, s, isomer 1 or 2), 7.39 (1H, s, isomer 1 or 2); MS ( $\text{ES}^+$ ) 405.1 (100%,  $[\text{M}+\text{H}]^+$ ); HRMS found  $[\text{MH}]^+$  405.1702,  $\text{C}_{25}\text{H}_{24}\text{O}_5$  requires  $[\text{MH}]^+$  405.1697.

**4.2.6.12. 2,3-Bis(4-methoxyphenyl)-1-(3,4,5-trimethoxyphenyl)prop-2-en-1-one 13l.** Thick yellow oil (88%, two isomers, ratio ~2:1);  $\delta_{\text{H}}/\text{ppm}$  (400 MHz,  $\text{CDCl}_3$ ) 3.73 (3H, s, isomer 1), 3.77 (3H, s, isomer 2), 3.78 (6H, s, isomer 1), 3.79 (3H, s, isomer 1),

3.82 (6H, s, isomer 2), 3.87 (3H, s, isomer 1), 3.88 (3H, s, isomer 2), 3.90 (3H, s, isomer 2), 6.73 (2H, d, *J* 8.8 Hz, isomer 1; 2H, d, *J* 8.8 Hz, isomer 2), 6.87 (2H, d, *J* 9.2 Hz, isomer 1), 6.90 (2H, d, *J* 8.6 Hz, isomer 2), 7.05 (2H, s, isomer 2), 7.06 (H, s, isomer 1), 7.10 (2H, d, *J* 8.6 Hz, isomer 2), 7.21 (2H, d, *J* 9.2 Hz, isomer 1), 7.19–7.26 (3H, m, isomer 2), 7.28 (2H, s, isomer 1), 7.35 (2H, d, *J* 8.8 Hz, isomer 1); MS ( $\text{ES}^+$ ) 435.1 (100%,  $[\text{M}+\text{H}]^+$ ); HRMS found  $[\text{MH}]^+$  435.1812,  $\text{C}_{26}\text{H}_{26}\text{FO}_6$  requires  $[\text{MH}]^+$  435.1802.

**4.2.6.13. 3-(3-Hydroxy-4-methoxyphenyl)-3-methoxyphenyl-1-(3,4,5-trimethoxyphenyl)prop-2-en-1-one 13m.** Thick yellow oil (90%, two isomers, ratio ~5:4);  $\delta_{\text{H}}/\text{ppm}$  (400 MHz,  $\text{CDCl}_3$ ) 3.78 (6H, s, isomer 1), 3.79 (6H, s, isomer 2), 3.79 (3H, s, isomer 1), 3.80 (3H, s, isomer 2), 3.82 (3H, s, isomer 1), 3.83 (3H, s, isomer 2), 3.87 (3H, s, isomer 1), 3.90 (3H, s, isomer 2), 6.64–6.90 (2H, isomer 1; 5H, isomer 2), 6.78 (1H, dd, *J* 1.8; 8.6 Hz isomer 1), 6.86 (2H, d, *J* 8.8 Hz, isomer 1), 7.00 (1H, s, isomer 1), 7.06 (2H, s, isomer 2), 7.16 (1H, s, isomer 2), 7.20 (2H, d, *J* 9.2 Hz, isomer 2), 7.27 (2H, s, isomer 1), 7.34 (2H, d, *J* 8.8 Hz, isomer 1); MS ( $\text{ES}^+$ ) 451.1 (100%,  $[\text{M}+\text{H}]^+$ ); HRMS found  $[\text{MH}]^+$  451.1755,  $\text{C}_{26}\text{H}_{26}\text{O}_7$  requires  $[\text{MH}]^+$  451.1751.

**4.2.6.14. 3-(4-Methoxy-3-nitrophenyl)-2-(4-methoxyphenyl)-1-(3,4,5-trimethoxyphenyl)prop-2-en-1-one 13n.** Thick yellow oil (67%, two isomers, ratio ~4:1);  $\delta_{\text{H}}/\text{ppm}$  (400 MHz,  $\text{CDCl}_3$ ) 3.77–3.90 (15H, isomer 1; 15H, isomer 2), 6.86–6.90 (3H, m, isomer 1; 3H, m, isomer 2), 6.98 (1H, s, isomer 2), 7.04 (2H, s, isomer 1), 7.08 (1H, s, isomer 1), 7.16 (2H, d, *J* 9.2 Hz, isomer 1), 7.22 (2H, s, isomer 2), 7.27 (1H, dd, *J* 1.6; 9.2 Hz, isomer 1), 7.35 (2H, d, *J* 8.8 Hz, isomer 2), 7.42 (1H, dd, *J* 1.6; 8.6 Hz, isomer 2), 7.64 (1H, d, *J* 1.6 Hz, isomer 1), 7.76 (1H, d, *J* 1.6 Hz, isomer 2); MS ( $\text{ES}^+$ ) 480.1 (55%,  $[\text{M}+\text{H}]^+$ ); HRMS found  $[\text{MH}]^+$  480.1652,  $\text{C}_{26}\text{H}_{25}\text{NO}_8$  requires  $[\text{MH}]^+$  480.1653.

**4.2.6.15. 3-(3-Fluoro-4-methoxyphenyl)-2-(4-methoxyphenyl)-1-(3,4,5-trimethoxyphenyl)prop-2-en-1-one 13o.** Thick yellow oil (67%, two isomers, ratio ~10:7);  $\delta_{\text{H}}/\text{ppm}$  (400 MHz,  $\text{CDCl}_3$ ) 3.78–3.80 (12H, isomer 1; 9H, isomer 2), 3.84 (3H, s, isomer 2), 3.87 (3H, s, isomer 1), 3.88 (3H, s, isomer 2), 6.74–7.01 (4H, m, isomer 1; 5H, m, isomer 2), 6.97 (2H, d, *J* 7.4 Hz, isomer 1), 7.04 (2H, s, isomer 2), 7.12 (1H, s, isomer 2), 7.17 (2H, d, *J* 7.2 Hz, isomer 2), 7.25 (2H, s, isomer 1), 7.33 (2H, d, *J* 7.4 Hz, isomer 1); MS ( $\text{ES}^+$ ) 453.1 (100%,  $[\text{M}+\text{H}]^+$ ); HRMS found  $[\text{MH}]^+$  453.1716,  $\text{C}_{26}\text{H}_{25}\text{FO}_6$  requires  $[\text{MH}]^+$  453.1708.

## 4.3. Biological evaluation

### 4.3.1. Cell inhibitory properties

Cells were cultured in RPMI medium, free of antibiotics and containing 2-mercaptoethanol (2  $\mu\text{M}$ ) and L-glutamine (2  $\mu\text{M}$ ), supplemented with foetal calf serum (FCS) (10% v/v). At monthly intervals all cell lines were inspected for mycoplasma contamination by the staff of the Paterson Institute. The cells were adjusted to a concentration depending on their observed doubling time (ca. 2000 cells/mL), in RPMI medium supplemented with FCS (10% v/v). The candidate drug was dissolved in DMSO. To 4 mL of cell solution was added 4  $\mu\text{L}$  of the drug solution and 1 mL of this solution was added to 1 mL of cell solution in the adjacent tube, giving a drug concentration half that of the first dilution. This series of dilutions was continued to afford seven samples at different concentrations leaving one cell solution free of drug acting as a control. Aliquots of 200  $\mu\text{L}$  of the treated cells were then pipetted in triplicate into a 96-well microtitre testplate and incubated (37 °C, 5%  $\text{CO}_2$  in air) for 5 days. After this time, the plate was removed from the incubator and 50  $\mu\text{L}$  of a solution of MTT (3 mg/mL in PBS) was added to each well. After incubation (37 °C, 5%

CO<sub>2</sub> in air, 3 h) the medium was carefully removed from each well by suction and the resulting formazan precipitate was dissolved in 200 µL of DMSO. The optical density of each well was then read at two wavelengths (λ 540 and 690 nm) using a Titretek Multiscan MCC/340 platereader. After processing and analysis through the application of an 'in-house' software package, the results obtained enabled the calculation of the drug dose required to inhibit cell growth by 50% (IC<sub>50</sub> value), determined by graphical means as a percentage of the control growth.

#### 4.3.2. Tubulin assembly assay

Six samples were prepared directly in quartz cuvettes at 0 °C and contained Mes buffer [740 µL (0.1 M Mes, 1 mM EGTA, 0.5 mM MgCl<sub>2</sub>, distilled water, pH 6.6)], GTP (10 µL, 100 mM in Mes buffer), tubulin (150 µL, 10–15 µM in Mes buffer) and the candidate drug (10 µL in DMSO). The tubulin/drug samples were immediately placed in a Varian Cary Bio 300 UV/visible spectrophotometer, preheated at 37 °C, alongside six blank samples containing Mes buffer (890 µL), GTP (100 µL) and the drug in DMSO (10 µL). Recording the absorbance (λ 350 nm) for a period of 30 min, the results were compared to the untreated control cells to evaluate the relative degree of change in optical density.

#### 4.3.3. Flow cytometry

To K562 cells in RPMI medium supplemented with FCS (10% v/v) (10 mL, 2 × 10<sup>5</sup> cells/mL) was added the candidate drug (10 µL, 5000 × IC<sub>50</sub> in DMSO). After incubation (37 °C, 5% CO<sub>2</sub> in air, overnight) the cells were centrifuged (1800 RPM, 10 min) and the supernatant discarded. The resulting pellet was re-suspended in a cold 1:1 mixture of acetone:ethanol (10 mL) and the mixture was stored at 4 °C until analysis was performed. The fixed cells were centrifuged (1800 rpm, 10 min) and the supernatant discarded. The resulting cell pellet was re-suspended in ice-cold PBS (10 mL) and centrifuged (1800 rpm, 10 min), again the supernatant discarded. The next stage involved the incubation (37 °C, 15 min) of the cells with RNase (150 µL, 100 µg/mL in PBS, DNase free, from bovine pancreas). The cell pellet was dissolved a solution of propidium iodide (0.25 mL, 50 µg/mL in PBS) and transferred to flow cytometry tubes before analysis by flow cytometry. The intracellular fluorescence was measured in a Coulter Epics V flow cytometer, using an argon laser (λ<sub>ex</sub> 488 nm).

#### Acknowledgments

The authors would like to acknowledge financial support from BBSRC (106/B18017, B18009 and BB/C524389/1) for postdoctoral fellowships for G.M., B.G. and J.F., a GTA award from UoS for E.B., a Bourse Innovation from the Conseil Régional d'Auvergne and Fonds européen de développement regional (FEDER) for J.F. and the Emerson Center for Scientific Computing (Emory University) for a visiting fellowship award for S.D. We thank the EPSRC National Mass Spectrometry Service Centre for HRMS. We are also

grateful to Prof. Dennis C. Liotta (Emory University) for generous assistance and hospitality during the course of the work.

#### References and notes

- Hadfield, J. A.; Ducki, S.; Hirst, N.; McGown, A. T. Tubulin and Microtubules as target for Anticancer Drugs. In *Progress in Cell Cycle Research*; Meijer, L., Jezequel, A., Roberge, M., Eds.; Kluwer Academic Plenum Publishers, 2003; Vol. 5, pp 309–325.
- Chaplin, D. J.; Hill, S. A.; Dougherty, G. J.; Prise, V. E.; Tozer, G. M.; Pettit, R. *Human Gene Ther.* **1999**, *10*, 840.
- Hill, S. A.; Tozer, G. M.; Pettit, G. R.; Chaplin, D. J. *Anticancer Res.* **2002**, *22*, 14538.
- Marx, M. A. *Exp. Opin. Ther. Pat.* **2002**, *12*, 769.
- Siemann, D. W.; Chaplin, D. J.; Walicke, P. A. *Exp. Opin. Invest. Drugs* **2009**, *18*, 189.
- Leoni, L. M.; Hamel, E.; Genini, D.; Shih, H.; Carrera, C. J.; Cottam, H. B.; Carson, D. A. *J. Natl. Cancer. Inst.* **2000**, *92*, 217.
- Ducki, S. *Idrugs* **2007**, *10*, 42–46.
- Ducki, S.; Hadfield, J. A.; Lawrence, N. J.; Liu, C. Y.; McGown, A. T.; Zhang, X. G. *Planta Med.* **1996**, *62*, 185.
- Ducki, S.; Forrest, R.; Hadfield, J. A.; Kendall, A.; Lawrence, N. J.; McGown, A. T.; Rennison, D. *Bioorg. Med. Chem. Lett.* **1998**, *8*, 1051.
- Lawrence, N. J.; McGown, A. T.; Ducki, S.; Hadfield, J. A. *Anti-Cancer Drug Des.* **2000**, *15*, 135.
- Nogales, E.; Wolf, S. G.; Downing, K. H. *Nature* **1998**, *391*, 199.
- Ravelli, R. B. G.; Gigant, B.; Curmi, P. A.; Jourdain, I.; Lachkar, S.; Sobel, A. *Nature* **2004**, *428*, 198.
- Ducki, S.; Mackenzie, G.; Lawrence, N. J.; Snyder, J. P. *J. Med. Chem.* **2005**, *48*, 457.
- Polanski, J. *Acta Biochim. Pol.* **2000**, *47*, 37–45.
- Uppuluri, S.; Knipling, L.; Sackett, D. L.; Wolff, J. *Proc. Natl. Acad. Sci. U.S.A.* **1993**, *90*, 11598.
- ter Haar, E.; Rosenkranz, H. S.; Hamel, E.; Day, B. W. *Bioorg. Med. Chem.* **1996**, *4*, 1659.
- Lowe, J.; Li, H.; Downing, K. H.; Nogales, E. *J. Mol. Biol.* **2001**, *313*, 1045.
- Morris, G. M.; Goodsell, D. S.; Halliday, R. S.; Huey, R.; Hart, W. E.; Belew, R. K.; Olson, A. J. *J. Comput. Chem.* **1998**, *19*, 1639.
- Cerbai, G.; Turbanti, L.; Bianchini, P.; Bramanti, G.; Tellini, N. *Boll. Chim. Farm.* **1967**, *106*, 837.
- Andreu, J. M.; Perez-Ramirez, B.; Gorbunoff, M. J.; Ayala, D.; Timasheff, S. N. *Biochemistry* **1998**, *37*, 8356.
- Chaudhuri, A. R.; Seetharamalu, P.; Schwarz, P. M.; Hausheer, F. H.; Luduena, R. F. *J. Mol. Biol.* **2000**, *303*, 679.
- Cortese, F.; Bhattacharyya, B.; Wolff, J. *J. Biol. Chem.* **1977**, *252*, 1134.
- Dumortier, C.; Yan, Q. Y.; Bane, S.; Engelborghs, Y. *Biochem. J.* **1997**, *327*, 685.
- Pettit, G. R.; Singh, S. B.; Hamel, E.; Lin, C. M.; Alberts, D. S.; Garciakendall, D. *Experientia* **1989**, *45*, 209.
- Tron, G. C.; Pirali, T.; Sorba, G.; Pagliai, F.; Busacca, S.; Genazzani, A. A. *J. Med. Chem.* **2006**, *49*, 3033.
- Woods, J. A.; Hadfield, J. A.; Pettit, G. R.; Fox, B. W.; McGown, A. T. *Br. J. Cancer* **1995**, *71*, 705.
- Simoni, D.; Romagnoli, R.; Baruchello, R.; Rondanin, R.; Rizzi, M.; Pavani, M. G.; Alloatti, D.; Giannini, G.; Marcellini, M.; Riccioni, T.; Castorina, M.; Guglielmi, M. B.; Bucci, F.; Carminati, P.; Pisano, C. *J. Med. Chem.* **2006**, *49*, 3143.
- Brown, R. T.; Fox, B. W.; Hadfield, J. A.; McGown, A. T.; Mayalarp, S. P.; Pettit, G. R.; Woods, J. A. *J. Chem. Soc., Perkin Trans. 1* **1995**, 577.
- Nandy, P.; Banerjee, S.; Gao, H.; Hui, M. B. V.; Lien, E. J. *Pharm. Res.* **1991**, *8*, 776.
- Kong, Y.; Grembecka, J.; Edler, M. C.; Hamel, E.; Mooberry, S. L.; Sabat, M.; Rieger, J.; Brown, M. L. *Chem. Biol.* **2005**, *12*, 1007.
- Pandit, B.; Sun, Y. J.; Chen, P.; Sackett, D. L.; Hu, Z. G.; Rich, W.; Li, C. L.; Lewis, A.; Schaefer, K.; Li, P. K. *Bioorg. Med. Chem.* **2006**, *14*, 6492.
- Nguyen, T. L.; McGrath, C.; Hermone, A. R.; Burnett, J. C.; Zaharevitz, D. W.; Day, B. W.; Wipf, P.; Hamel, E.; Gussio, R. *J. Med. Chem.* **2005**, *48*, 6107.
- Peyrot, V.; Leynadier, D.; Sarrazin, M.; Briand, C.; Menendez, M.; Laynez, J.; Andreu, J. M. *Biochemistry* **1992**, *31*, 11125.